TRANSCRIPTIONAL EFFECTS OF PREDATOR CUES IN THE BRAIN OF *SPODOPTERA FRUGIPERDA* (LEPIDOPTERA: NOCTUIDAE) MOTHS EXPOSED TO BAT ULTRASOUND

BY

SCOTT DOMINIC CINEL

THESIS

Submitted in partial fulfillment of the requirements
for the degree of Master of Science in Entomology
in the Graduate College of the
University of Illinois at Urbana-Champaign, 2016

Urbana, Illinois

Master's Committee:

Dr. Steven J. Taylor, Chair, Director of Research
Professor May R. Berenbaum
Associate Professor Alison M. Bell
Assistant Professor Brian F. Allan

ABSTRACT

Exposure to predators induces broad behavioral and physiological responses that have traditionally been considered acute and transitory. However, prolonged frequent exposure to predators and the chemical, visual, tactile, and auditory cues they broadcast to the environment are now known to have long-term impacts on prey physiology and life-histories. Knowledge on the molecular mechanisms responsible for inducing both acute and chronic responses to predator exposure is limited. Although several studies have assessed acute and chronic stress responses in a variety of taxa, these efforts have often involved *a priori* expectations of the molecular pathways involved in the physiological response, such as glucocorticoid and neurohormone production. While relatively little is known about physiological and molecular predator-induced stress responses in insects, many dramatic defensive behaviors in insects have been reported. Within several moth families, such as Noctuidae, tympanic organs for recognizing ultrasonic bat calls have evolved and facilitate the avoidance of predation via eliciting flight cessation or aerial maneuvers when stimulated by ultrasound. In this study, I exposed adult male fall armyworm (*Spodoptera frugiperda*) moths to recorded ultrasonic bat foraging and attack calls for a prolonged period and constructed a *de novo* transcriptome using RNA-Seq on mRNA extracted from the brains of predator-exposed and unexposed moths. I then identified differentially-expressed transcripts between the exposed and control groups and used functional gene analysis and Gene Ontology (GO) enrichment analysis to reveal that the majority of differentially expressed transcripts corresponded to a broad range of proteins involved in cellular processes in the brain, including glutamate production and metabolism, ionotropic sensory receptor expression, mitochondrial metabolism, actin cytoskeleton dynamics, chromatin binding and other epigenetic modifications, axonal guidance and remodeling, cilia function and development, Wnt

signaling, and TOR signaling. The top five significantly over-represented GO terms included chromatin binding, macromolecular complex binding, glutamate synthase activity, glutamate metabolic process, and glutamate biosynthetic process. Although limited by a *de novo* approach, this study demonstrates that predator-induced transcriptional responses in *S. frugiperda* vary broadly in their physiological and molecular functions. As a first assessment of auditory predator cues on transcriptional responses in moth prey, this study also lays the foundation for future research on the complex array of integrated behavioral, physiological, and cellular responses to predators observed in ultrasound-sensitive Lepidoptera.

To my mother and father,

who first taught me about the intricacies of the natural world.

"When we try to pick out anything by itself,

we find it hitched to everything else in the Universe."

- John Muir

ACKNOWLEDGMENTS

First, I would like to acknowledge and thank Dr. Inga Geipel and Dr. Kirsten Jung for their assistance in procuring the recorded ultrasonic bat calls used in this thesis. I would also like to thank Dr. Daniel Llano and Gosha Yudintsev for providing ultrasonic loudspeakers used in this study and for allowing me access to their sound-proof chambers. My thanks also go to Dr. May Berenbaum, Daniel Bush, and Luke Zehr for their assistance with diet preparation and for advice on rearing *Spodoptera frugiperda*. I also thank Dr. Mark Davis, Dr. Matt Niemiller, Dr. Amy Cash Ahmed, Ian Traniello, and Beryl Jones for their logistic support during the dissection and RNA extraction processes. I thank Dr. Jenny Drnevich, Dr. Alvaro Hernandez, Dr. Chris Fields, and Evan McCartney-Melstad for their consultations regarding many bioinformatic technicalities throughout this work. Dr. Steven J. Taylor, Dr. May Berenbaum, Dr. Alison Bell, Dr. Brian Allan, Dr. Rachel Page, and Dr. Owen McMillan were instrumental in the intellectual development of this project, especially during its early stages, and deserve my utmost gratitude. Finally, I would like to thank the National Science Foundation, the Smithsonian Tropical Research Institute, the University of Illinois' Office of External Fellowships, the School of Integrative Biology at the University of Illinois at Urbana-Champaign, and its faculty involved in managing the IGERT Vertically Integrated Training in Genomics Fellowship and smaller research awards, which financially supported most of this study.

TABLE OF CONTENTS

INTRODUCTION.....1

METHODS.....10

RESULTS.....19

DISCUSSION.....22

REFERENCES.....37

TABLES AND FIGURES.....59

INTRODUCTION

Predator-Induced Stress and its Influences on Prey Behavior, Physiology, and Demography

Predator-induced responses in prey organisms have, until recently, been viewed as acute and transitory, with minimal lasting impact on physiology or population demographics (Clinchy *et al.*, 2013). Prey undergo adaptive responses simply in the presence of predators by integrating auditory, visual, or chemosensory cues (Barks *et al.*, 2013; Breviglieri *et al.*, 2013; Van Buskirk *et al.*, 2013), often initiating a suite of behavioral and physiological responses that contribute to the prey's ability to survive encounters with predators. However, fear factors significantly into ecological theory, with predator-induced behavioral changes contributing to patterns of optimal foraging and game theory (Brown *et al.*, 1999). In fact, Walter B. Cannon, one of the first to study predator-induced stress in wildlife, stated in 1915: "The increase in blood sugar, the secretion of adrenin [*sic*] and the altered circulation in pain and emotional excitement have been interpreted… as biological adaptations to conditions in wildlife which are likely to involve pain and emotional excitement, i.e., the necessities of fighting or flight… The cornering of an animal when in the headlong flight of fear may suddenly turn the fear to fury and the flight to a fighting in which all the strength of desperation is displayed" (Cannon, 1915).

The concept of an acutely stressful period associated with a fight-vs.-flight response has been prevalent in ecological and physiological research for decades, exemplified by Hawlena and Schmitz's (2010) review of studies assessing acute stress responses in both wild and laboratory-reared animals, in which they document how acute encounters with a predator initiate physiological responses, usually on the scale of a few minutes to several hours post-exposure. These responses include increased respiration rates, heart rates, and ventilation, along with elevated hemolymph/blood heat shock protein (Hsp) levels in aquatic invertebrates (Pauwels *et al.*, 2005; Rovero *et al.*, 2000) and fish (Kagawa *et al*, 2009), and increased blood

glucocorticosteroid (GCS) levels in fish (Cooke *et al.*, 2003; Kagawa *et al.*, 2009), mammals (Eilam *et al.*, 1999; Hubbs *et al.*, 2000), reptiles (Thaker *et al.*, 2009), and birds (Cockrem and Silverem, 2002).

However, Hawlena and Schmitz (2010) also admit that "[e]xposure to long-lasting stressors (e.g., chemical cues of predator presence) or frequent exposure to acute stressors (e.g., predator attack) … may prevent the attenuation of stress hormones and Hsps to pre-exposure levels. This leads to prolonged inhibition of essential nonemergency body functions, accumulations of destructive effects on molecular and cellular structure and functions, and nutritional imbalance." Several other studies have assessed the physiological impacts of chronic predation risk, occurring on the scale of several days to the lifetime of the organism, and found similar increases in stress hormone and behavioral reactions induced during acute responses but for extended periods of time (Beckerman *et al.*, 2007; Clinchy *et al.*, 2004; Monclus *et al.*, 2009; Polednik *et al.*, 2008), along with significant reductions in antioxidant enzyme levels (Slos and Stoks, 2008). In part due to the long-held and compelling understanding of acute fight-vs.-flight responses on physiology, Clinchy *et al.* (2010) argue two main reasons for why prolonged exposure to long-lasting stressors or frequent acute stressors, i.e. chronic stressors, has not been assessed until relatively recently: 1) comparative physiologists have assumed that predator-induced stress is inherently transitory, with no effect on chronic stress, and 2) those interested in studying predator-prey ecology have also largely ignored predator-induced stress while focusing on the impacts of predation on population size. Demographic parameters, such as reproduction and disease, occurring at longer time scales relative to direct predator-prey interactions, have been attributed largely to chronic physical challenges, i.e., shortages of food, rather than to predator-induced stress (Krebs, 2002; Creel and Christianson, 2008). Several lines of evidence

have emerged that suggest predators have a much broader impact on prey, affecting broad adaptive responses which can impact demographic processes, such as reproduction, and long-term physiological and behavioral responses, such as metabolic activity and changes in escape maneuvers in response to predators. Indeed, chronic exposure to predators modified so as to be nonlethal induces plastic behavioral responses in several prey organisms, allowing for more time to escape and enhanced escape responses (Hawlena *et al.,* 2011; Miller *et al.,* 2014). For instance, *Melanoplus femurrubrum* grasshoppers reared within field enclosures along with modified hunting spiders, which had their chelicerae glued together, initiated escape responses 1.2 times faster and jumped 2.6 times farther than grasshoppers reared without any real or perceived predation risk (Hawlena *et al.,* 2011).

The fact that predators can alter prey demography through killing is one of the fundamental tenets of predator-prey ecology, yet ecologists have acknowledged since the 1990s that direct mortality by predators cannot account fully for patterns in prey demography (Krebs *et al.* 1995, Peckarsky *et al.,* 1993). For instance, Peckarsky *et al.* (1993) investigated the sublethal effects of predatory stoneflies on mayfly demographics. By using field enclosure experiments with mayfly naiads, Peckarsky *et al.* (1993) compared feeding rates, growth rates, and fecundity under predation risk from two species of stoneflies, the second of which had its mouthparts glued shut, representing nonlethal predation risk. Under both predation risk regimes, mayfly naiads matured at reduced sizes relative to those with ample food but no predator exposure and displayed a similar mature size to naiads held in low resource conditions. Moreover, female mayflies under predation risk exhibited reduced egg mass but allocated a similar proportion of total body mass to eggs as those under no risk of predation. These patterns clearly indicate that both real and perceived predation risk influences the growth and fitness of mayfly naiads. A

similar phenomenon was observed by Krebs *et al.* (1995) using predator exclosure experiments on snowshoe hare populations for eight years. Predator exclosure and food addition combined resulted in an 11-fold increase in hare population increase while these effects individually accounted for only two- and three-fold increases, respectively, which may indicate that predation risk affected hares indirectly by inhibiting them from optimally utilizing available resources. While these cases demonstrate that nonlethal effects of predation significantly alter demographic parameters of both insects and mammals, these responses may also be attributed to reduced food intake and disrupted foraging opportunities during interactions with predators (Mella *et al.*, 2014).

Controlled field studies have contributed to decoupling these alternate hypotheses in mammals and birds (Sheriff, *et al.* 2009; Travers *et al.*, 2010). Sheriff *et al.* (2009) exposed caged pregnant snowshoe hares with ample access to food to a trained dog and observed elevated fecal glucocorticoid levels along with significantly reduced numbers of successful births in exposed females. A follow-up study (Sheriff *et al.*, 2011) assessed physiological stress responses in the same species of hare during a 10-year population cycle. During years with high densities of predators, hares had enhanced levels of plasma and fecal glucocorticoids, an increased ability to mobilize energy, and poorer visible body condition. Furthermore, Travers *et al.* (2010) found that song sparrows which experienced experimental nest predation in the form of removal of all of their eggs produced fewer eggs in their next nest relative to sparrows that experienced producing an unviable clutch by using artificial egg replacements. Travers *et al.* (2010) also found that physiological dysregulation, measured via multivariate analysis based on glucocorticoid, antioxidant, and oxidative stress levels, was nearly three times greater in the birds that underwent nest predation. Indeed, Cantor (2009) argues that these physiological and

behavioral responses to predators are conserved across taxa and have guided development of brain and sensory structures that aid in mediating responses to predatory signals in the environment.

In insects, exposure to lethal and nonlethal predators (Adamo *et al.,* 2013) and simple non-predatory disturbances (Chen *et al.,* 2008; Even *et al.,* 2012) can elicit up-regulation of stress-related genes that help modulate behavior, metabolism, and cellular stress in response to predator exposure (Aruda *et al.*, 2011; Slos and Stoks, 2008). Current understanding of these genes is limited but they are thought to play a role in the production of gene products responsible for the enhanced arousal, vigilance, and metabolic activity associated with predator exposure (Arun, 2004). For instance, the neuropeptide octopamine induces anti-predatory behavior similar to that observed under prolonged predator exposure in the cricket *Gryllus texensis* (Adamo *et al.,* 2013). Additionally, metabolic neurohormones and neuropeptides, such as adipokinetic hormone (AKH), diuretic hormone (DH), allatostatin (ATN), corazonin (CZN), and juvenile hormone (JH) have been associated with increased fat metabolism, heart rate, nutrient absorption, water excretion, and other physiological processes that may be related to producing functional predator-induced behavioral responses in prey (Even *et al.*, 2012; Gäde *et al.,* 2008). Furthermore, several neuropeptides and antioxidant enzymes act as chaperones during episodes of cellular stress and help protect cells from oxidation and protein misfolding that may result from increased metabolic demand during predator-prey interactions (Even *et al.,* 2012; Fleshner *et al.*, 2004; Peric-Mataruga *et al.,* 2006). For instance, in *Helicoverpa armigera*, a noctuid moth, ultrasound exposure induces a significant increase in peroxidase activity 40 minutes post-exposure in both larvae and adults (Zha *et al.* 2013). These and other active products of genes may help modulate prey responses to direct and indirect predator exposure.

The Ultrasonic Arms Race Between Bats and Eared Moths

The ability to perceive airborne sounds has evolved independently in at least nine insect orders including Orthoptera, Mantodea, Blatodea, Hemiptera, Hymenoptera, Coleoptera, Neuroptera, Lepidoptera, and Diptera (Gopfert and Hennig, 2016). Presumably, this ability evolved for the purpose of acoustic communication, operating over large distances in structurally complex habitats (Romer and Bailey, 1996) and for the acoustic detection of predators (Conner and Corcoran, 2012). The main predators of nocturnal flying insects are aerial hawking insectivorous bats (Yangochiroptera) which first appear in the fossil record around 65 million years ago. This novel aerial predator placed strong selective pressure on nocturnal flying insects (Conner and Corcoran, 2012) which had occupied a relatively predator-free niche since their concurrent evolution with reptiles and largely diurnal birds around 300 million years ago (Organ *et al.,* 2008). Subsequently, this new predator-prey interaction placed significant predation pressure on nocturnal flying insects, with recent studies indicating that bat predation accounts for the majority of predation-related nocturnal flying insect mortality (Kalka *et al.,* 2008). Longstanding studies of auditory mechanisms in insects, including disparate taxa such as tiger beetles (Spangler, 1988) and mantises (Yager *et al.*, 1990), have revealed that many taxa possess functional ear-like particle-velocity-sensitive antennal organs, tympanal organs, or even atympanate structures (Gopfert and Hennig, 2016) that allow the discrimination of both intra- and inter-specific auditory cues (Hedwig, 2016; Pfuhl *et al.*, 2015; Rowland *et al.*, 2014). Indeed, auditory sensory organs in insects provide precise auditory recognition, mechanical amplification, directionality, intensity fractionation, and frequency decomposition capabilities that rival peripheral sound processing in vertebrates (Gopfert and Hennig, 2016).

The distribution of these capabilities is not, however, universal throughout Class Insecta. For instance, sound-sensitive Lepidoptera are, for the most part, unable to discriminate between sound frequencies, as their tympanal membranes generally resonate in response to a specific ultrasonic frequency range and are innervated by only one to four neurons (Pfuhl *et al.*, 2015). Despite this, even tiny moths, which cannot rely on interaural intensity differences experienced by the ears of larger moths, are able to respond directionally to a sound (Surlykke, 1984; Greenfield *et al.*, 2002; Pfuhl *et al.*, 2015). The predominant hypothesis for explaining the evolution of bat-responsive tympanal organs suggests that most taxa co-opted ancestral chordotonal receptors (Pfuhl *et al.*, 2015) for use first in sexual signaling and intraspecific communication and then in detection of predators (Yager and Svenson, 2008). Among these taxa, night-flying Lepidoptera faced with this new predator evolved an auditory mechanism capable of hearing bat ultrasound and generating appropriate behavioral and physiological responses to avoid predation (Roeder, 1965).

Using tympanal organs situated on the posterolateral edges of the metathorax, adult noctuid moths are well-known detectors of bat ultrasound (Waters and Jones, 1996; Roeder, 1998). Each tympanum is innervated by three neurons: the A1 and A2 cells, which respond to ultrasound in an excitatory manner, and the B cell, which is a putative proprioceptor (Surlykke and Miller, 1982). This simple noctuid auditory system, comprising just these three sensory neurons, is considered one of the simplest found in nature and has served as a model for anti-predator neuroethology studies for decades (Fullard *et al.*, 2003). The A1 and A2 afferent neurons have ramifications in the meso- and meta- thoracic ganglia, connecting to several abdominal, thoracic, and brain interneurons. Notably, one subset of sound-sensitive repeater interneurons extends from the thoracic ganglia to a neuropil in the ventro-lateral protocerebrum

(VLPC) (Pfuhl *et al.*, 2015), a section of the noctuid brain that Roeder (1966) found was sensitive to sound as well. The VLPC may be a higher-order neuropil involved in multimodal sensory integration, as sound-sensitive brain interneurons (Pfuhl *et al.*, 2014) and a descending sound-sensitive neuron (Olberg and Willis, 1990) have ramifications in this region. Upon exposure to ultrasound, non-flying noctuids cease movement while many aerial noctuids exhibit evasive flight maneuvers, such as erratic changes in direction, loops, increases in flight velocity, and even falling to the ground (Miller and Surlykke, 2001). Moreover, when exposed to bat calls, many female and male moths, including noctuids specifically, alter their mating behaviors, stopping pheromone release or ceasing flight, respectively (McNeil and Acharya, 1998). Though simplistic, these A1 and A2 neurons provide a distinct advantage to noctuid moths threatened by bat predation, as the more sensitive A1 informs the moth of bat presence while the less sensitive (15–20 dB higher threshold) A2 cell may induce behavioral escape maneuvers once a bat has approached within a certain distance (Fullard *et al.*, 2003; Gopfert and Hennig, 2016). These behavioral responses, especially when carried out for an extended time period, may contribute to patterns of stress-related gene regulation and peptide production in insects, perhaps leading to reported patterns of reduced fecundity and altered physiology of another noctuid moth species after exposure to recorded ultrasound (Zha *et al.*, 2008, 2013).

In this study, I searched for wide-ranging transcriptional effects of frequent, prolonged exposure to indirect predator cues in the brain of adult *Spodoptera frugiperda*, the fall armyworm moth. In an attempt to describe a holistic predator-induced stress response without a need for measuring *a priori* physiological parameters, such as discrete neuropeptide levels, we employed a *de novo* transcriptomic approach to differential gene expression analysis with RNA-Seq. Using recorded calls of foraging and attacking bats, I exposed one group of moths to the

calls while protecting a second group of moths from exposure to calls. Through comparison of brain tissue transcript expression profiles between these two groups, I aimed to identify those gene products whose transcription is most strongly induced or repressed during bat-moth interactions. Specifically, I hypothesized that exposure to recorded bat ultrasound would induce patterns of gene regulation related to the synthesis of neuropeptide hormones, metabolic hormones, neurotransmitters, antioxidant enzymes, and the associated receptor proteins for these products. Additionally, I hoped to uncover many other differentially expressed gene products and, through evaluation of their functions, develop novel perspectives on the stress physiology of these indirect predator cues.

METHODS

Rearing Fall Armyworm

Fall armyworm larvae were ordered from Frontier Agricultural Sciences (Newark, DE, USA) under USDA APHIS PPQ 526 permit (P526P-04080) and were received as second and third instars. Upon arrival, larvae were transferred to individual 59.15 mL plastic cups in which 10 - 15 mL of standard lepidopteran diet (see below) had been placed and reared in a dedicated environmental chamber (Percival Scientific, Perry, IA, USA) at 30 ± 1℃, 75 ± 5% relative humidity with a photoperiod cycle of 16 h light/8 h dark. Larvae fed *ad libitum* on modified standard lepidopteran larvae diet (Elvira *et al.*, 2010; Sims, 1998; Sorour *et al.*, 2011) prepared every two weeks. This diet consisted of the following: 13 g agar, 770 mL distilled water, 31.5 g vitamin-free casein, 24 g sucrose, 27 g wheatgerm, 9 g Wesson's salt mix, 10 g alphacel, 5 mL 4 M potassium hydroxide, 18 g Vanderzant's vitamins, 1.6 g sorbic acid, 1.6 g methyl paraben, 3.2 g ascorbic acid, 0.12 g streptomycin salt, 4 mL wheatgerm oil, and 2 mL 10% formaldehyde. I blended the casein, sucrose, wheatgerm, Wesson's salt mix, Alphacel, 220 mL distilled water, and potassium hydroxide on a high setting for 5 minutes, after which I added 550 mL of distilled, deionized (DDI) water mixed with the agar and heated just until boiling. This mixture was then blended for another 5 min and allowed to cool to 60℃ before adding the Vanderzant's vitamins, sorbic acid, methyl paraben, ascorbic acid, streptomycin, wheatgerm oil, and formaldehyde and then blending for a final 5 minutes. Between 10 and 15 mL of the diet was placed into each rearing cup and allowed to solidify in a cold-room.

Neonates were placed into individual cups fitted with a lid in which two holes had been punched using a No. 1 insect pin. Once each larva matured and cleared its gut in preparation for pupation, I transferred it to a shallow Tupperware© container (29.4 cm x 15.1 cm x 10.5 cm)

filled with 3.5 cm of loose potting soil (SunGro Horticulture, Vancouver, Canada). Once per day, this soil was sifted gently by hand to extract any pupae, which were placed in a separate 30.48 cm cube-shaped mesh cage (BioQuip Products, Inc., Compton, California, USA) with a mesh-size of 51.15 holes/cm^2, within the environmental chamber until emergence.

Upon emergence, adults were transferred to a similar mesh cage and allowed to mate. Twice daily, I saturated the sides of the mesh cage with a 10% sucrose solution to allow feeding. To avoid the possible confounding effects of shipment and the change in diet undergone by the generation of larvae received from Frontier Agricultural Sciences, F1 eggs were collected daily from within this cage and placed in small plastic containers within the rearing chamber. Once hatched, F1 larvae were reared individually as described until emergence as adults, after being segregated by sex as pupae.

Predator-Cue Exposure

F1 adult males (N = 8) were haphazardly selected for exposure trials 24–48 hours post-emergence; females were not used, as female moths broadcasting pheromones are much more sedentary (Stelinski *et al.*, 2014) and therefore may be less likely to be a target of attack by aerial-hawking bats. Three successive recordings of aerial insectivorous bat calls were used during predator exposure trials. These recordings were sampled at 480 kHz with a 16-bit format and include a 4.27 s *Mollosus mollosus* (Chiroptera: Molossidae) attack call and two foraging calls of 1.51 s and 2.92 s made by *Myotis nigricans* (Chiroptera: Vespertilionidae) and *Saccopteryx bilineata* (Chiroptera: Emballonuridae), respectively. These neotropical aerial-hawking species were selected as they represent novel predators to which the population of *S. frugiperda* I utilized had never possibly been exposed, yet broadcast foraging and attack calls at frequency ranges tuned to the noctuid tympanal organ (Jung *et al.*, 2007; Mora *et al.*, 2004;

Surlykke and Kalko, 2008). Furthermore, these three species broadcast at different ranges which together cover the spectrum of frequencies processed by noctuid tympanal organs, with *M. molossus*, *M. nigricans*, and *S. bilineata* broadcasting at 20–50 (Mora *et al.*, 2004), 50–85, and 45–55 (Jung *et al.*, 2007) kHz, respectively. The individual .wav sound files, courtesy of Dr. Kirsten Jung, were processed in Audacity v. 2.1.0. I reduced the background noise present in each raw file by applying a 20 dB noise reduction filter with moderate sensitivity (10.0) and downsampled each file to 195.3125 kHz sampling rate as this was the upper limit of our playback system. This downsampling, although attenuating auditory frequencies greater than 75 kHz (Tucker-Davis Technologies, personal communication), allowed frequencies of interest to be broadcast accurately and well within the 20-50 kHz optimal frequency range reported for noctuid moths (Fullard, 1988; Norman and Jones, 2000). These three calls were then concatenated into a single .wav file consisting of each factorial combination of playback order and 10 s of silence inserted between each of the calls (Fig. 1). Although the noctuid tympanal organ shows no signs of neuronal habituation, even when exposed to call rates up to 20 Hz (Boyan and Fullard 1986), I chose to separate each call with 10 s of silence to reduce the likelihood that habituation might occur. This 38 s file was then looped for the duration of each playback trial.

For each trial, a single male moth was placed within a mesh cage and the sound loop was broadcast from a Tucker-Davis Technologies (TDT, Alachua, Florida, USA) System 3, ES1 electrostatic free-field speaker (TDT) at 60 dB SPL situated externally 30 cm from the center of the cage in a soundproof room. The RPvdsEx software suite v. 80 (TDT) was used to process and playback the .wav files via a TDT RP2.1 processor, ED1 Electrostatic Speaker Driver, and SA1 Stereo Amplifier tandem setup. Each trial took place from 22:00 – 05:00, with a new set of

two males used on 4 consecutive nights. Each control exposure consisted of a single male moth in a mesh cage placed within a soundproof chamber from 22:00 – 05:00 but with no audio playback.

Tissue Dissection and RNA Stabilization

Immediately post-exposure at 05:00, each moth was placed into a 2 mL vial and immediately immersed in liquid nitrogen. After 30 s, the moth was removed from the vial and transferred quickly to a Petri dish on dry ice. The head was removed and immersed in RNAlater stabilization solution (Thermo Fisher Scientific, Waltham, Massachusetts, USA). Upon immersion, scales on the head capsule were removed by scraping with scalpel, and a 1 mm x 1 mm section of cuticle was cut to expose the brain tissue directly to RNAlater. We then removed the brain intact from the head capsule, rinsed it with fresh RNAlater solution, placed it in a 2 mL microtube of fresh RNAlater solution, and stored it at 2℃ until all samples had been collected.

RNA Extraction, Library Preparation, and Sequencing

RNA was extracted from each control (N = 4) and exposure (N = 4) brain individually using a PicoPure RNA Isolation Kit (Arcturus Bioscience, Inc., Carlsbad, California, USA) after extractions were treated with RNase-free DNase (Qiagen, Hilden, Germany). RNA was eluted in 30 uL of RNase-free water and stored at -80℃ until further analysis. Before freezing, 3.5 uL aliquots were removed from each extract and used for RNA quantification via a NanoDrop (Thermo Fisher Scientific, Waltham, Massachusetts, USA) spectrophotometer and a Qubit fluorometer (Thermo Fisher Scientific, Waltham, Massachusetts, USA) using a Qubit RNA HS Assay Kit (ThermoFisher Scientific, Waltham, Massachusetts, USA). After a 1:10 or 1:15 dilution based on each sample's concentration, I submitted these subsamples to the Functional Genomics Unit of the University of Illinois at Urbana-Champaign's (UIUC) Roy J. Carver

Biotechnology Center to confirm RNA quality with a Bioanalyzer RNA 6000 Pico chip (Agilent Technologies, Santa Clara, California, USA). I then submitted each sample to the UIUC Roy J. Carver Biotechnology Center's High-Throughput Sequencing and Genotyping Unit for library preparation and sequencing. Strand-specific cDNA libraries were prepared using an Illumina TruSeq Stranded mRNA Sample Prep Kit (dUTP based) according to manufacturer specifications and quantitated by quantitative polymerase chain reaction (qPCR). The eight samples were pooled on a single lane of an Illumina 2500 sequencer and the RNA fragments were sequenced using Illumina's HiSeq SBS Sequencing Kit v4 for 101 cycles with a 100 nt paired-end read length.

Raw mRNA Read Preprocessing

Sequence files in .fastq format were generated and demultiplexed with Illumina's bcl2fstq v. 217.1.14 conversion software. To attain raw read quality reports, I first ran FastQC v. 0.11.2 (Andrews, 2010) with default settings on each set of reads. I then preprocessed the raw reads by performing adapter trimming, quality filtering, and *in silico* normalization. Adapter trimming and quality filtering were achieved using Trimmomatic v. 0.33 (Bolger *et al.* 2014) in palindrome mode to search for and remove adapter sequences, low-quality bases from the leading and trailing ends of each read with phred scores less than 28, and reads shorter than 30 bases in length. To remove redundant reads and improve transcriptome assembly performance, the remaining reads were then digitally normalized to a coverage depth of 50x via the Trinity transcriptome assembly suite v. 2.1.1 (Grabherr *et al.*, 2011; Haas *et al.*, 2013).

De Novo Transcriptome Assembly, Annotation, and Quality Assessment

To date, there is no publicly-available annotated genome for *Spodoptera frugiperda*; therefore, I assembled a *de novo* transcriptome with the pre-processed reads using Trinity v.

2.1.1 (Grabherr *et al.*, 2011). I designated the sequence-specific strand orientation to 'reverse-forward' (RF) when selecting options for running Trinity, as this is the strand orientation produced by Illumina's TruSeq Stranded mRNA Sample Prep Kit. The quality of the resulting transcriptome was then assessed using TransRate v. 1.0.1 (Smith-Unna *et al.*, 2015). I then utilized the Annocript v. 0.2.30 automated transcriptome annotation software package (Musacchia *et al.*, 2015) to complete sequence-similarity searches based on our constructed transcriptome using BLAST+ v. 2.2.30. I chose to use the UniRef90 automated annotation database (UniProt Consortium, 2013) to screen for computationally-derived protein annotations. Annocript first downloaded the UniRef90 database, stored it in a MySQL (Oracle Corporation, Redwood City, CA, USA) database, and indexed it for faster searches (Camacho *et al.*, 2009). Annocript then carried out BLASTX searches against the UniRef90 database while keeping only those hits with an e-value < 1e-5. Annocript output a .gff3 (General Feature Format v. 3) tab-delimited feature map file containing the collated UniRef90 BLASTX matches and associated GO annotation information for each putative transcript within the *de novo* assembled transcriptome which we used for subsequent analyses. The raw sequence reads have been uploaded to the National Center for Biotechnology Information's (NCBI) Sequence Read Archive (SRA) database (accessions: SRR3406020, SRR3406031, SRR3406036, SRR3406052, SRR3406053, SRR3406054, SRR3406055, SRR3406059) and are also available through the BioProject accession PRJNA318819 (https://www.ncbi.nlm.nih.gov/bioproject/PRJNA318819). The *de novo* transcriptome assembly has been submitted to NCBI's Transcriptome Shotgun Assembly (TSA) database under accession GESP00000000 and the version described in this thesis is the first version, GESP01000000.

Read Alignment and Abundance Quantification

Following annotation, I indexed the transcriptome in preparation for alignment using STAR v. 2.5.0a (Dobin *et al.*, 2013) and each sample's preprocessed reads were then individually mapped to the assembly using STAR and output as unsorted .BAM files. I elected to call the '—outMultimapperOrder Random' option when running STAR to ensure that multi-mapped read alignments were output in random order and that the selection of a primary alignment was made randomly from the top scoring alignments. All other parameters were kept at their default values.

Next, I used these alignments to the *de novo* transcriptome as input, along with the raw reads, to quantify read counts using the software package Salmon v. 0.6.0 in alignment-based mode (Patro *et al.* 2015). When running Salmon, I designated that our paired reads were inward-facing and stranded, and that the first read of the pair came from the reverse strand, as is typical of output from Illumina's Stranded mRNA Sample Prep Kit. I also chose to let Salmon correct for random priming bias, which can result in certain nucleotide motifs being preferentially sequenced. Salmon produced expression estimates for each transcript in the transcriptome, which I then used in our downstream statistical analyses.

Differential Transcript Expression Analysis

In R v. 3.2.4 (R Core Team, 2016), I utilized the packages 'edgeR' v. 3.12.1 (Robinson *et al.*, 2010) and 'limma' v. 3.26.9 (Ritchie *et al.*, 2015) to input our read abundance estimates and perform differential expression analyses. First, I used the trimmed mean of M-values (TMM) normalization method (Robinson and Oshlack, 2010) to account for small differences in each sample's overall read library size. To filter out transcripts with low expression estimates carrying little or no useful information and thus reducing detection power for moderate to highly

expressed genes (Rau *et al.*, 2013), I calculated the counts per million (CPM) mapped reads for each transcript and removed those with CPM < 1.

I then assessed the presence of unexpected batch effects in the data by performing principal components analysis (PCA) on log-transformed CPM values for each sample using the 'affycoretools' v. 1.42.0 (MacDonald, 2008) package in R. To account for the large transcript expression variation observed between samples within the control and exposure groups, I used the 'sva' v. 3.18.0 (Leek *et al.*, 2010, 2015) package in R to explicitly model two significant surrogate variables, representing unexpected batch effects, as covariates. After adding these surrogate variables to our dataset manually, I log-transformed all CPM estimates to prepare the data for linear modeling. I then used the 'limma' package and its 'voom' function (Law *et al.*, 2014) to fit a negative binomial linear model to the data and proceeded to compute t-statistics, F-statistics, and log-odds of differential expression for each transcript using an empirical Bayes approach (Smyth, 2004). The resulting differentially-expressed transcripts were filtered by selecting only those with false discovery rate (FDR)-adjusted p-values < 0.05 and a fold-change > 2. I chose to use FDR-adjustment to account for multiple testing bias on p-value significance.

To produce a heatmap of gene expression for these transcripts across the samples, I scaled each transcript's associated fold-change to the mean fold-change observed in all transcripts from the control group. To assess similarity in expression between samples, I used a hierarchical clustering method based on a distance matrix compiled by taking the maximal distance between any two expression values in each sample via the 'fastcluster' package v. 1.1.20 (Mullner, 2013) in R. The resultant base dendrogram of similarity between individual transcripts was then used to identify the most appropriate level at which to cluster transcripts using the R package 'dynamicTreeCut' v. 1.63-1 (Langfelder *et al.*, 2008). I used the 'hybrid'

method to first identify large, base clusters following four criteria: 1) each cluster must contain at least two transcripts, 2) transcripts that are too distant from a cluster are excluded, even if they occur on the same branch, 3) each preliminary cluster must be distinct from those clusters near to it, and 4) the tips of each preliminary cluster must be tightly connected. Once these preliminary clusters were identified, any transcripts not previously assigned were placed in the closest cluster. Using 'cdbfasta' v. 0.99 (https://sourceforge.net/projects/cdbfasta/), I then retrieved the sequences and GO terms associated with these differentially-expressed (DE) transcripts from our annotated transcriptome and used them for downstream functional GO annotation.

All figures were constructed using the R packages 'graphics' v. 3.2.4, 'grDevices' v. 3.2.4, 'rgl' v. 0.95.1441, and 'gplots' v. 2.17.0.

GO Term Enrichment Analysis

To obtain a broader perspective on the function of our DE transcripts and how they may be related, I tested the transcripts and their associated annotated GO terms for statistically significant over- and under-representation via GO term enrichment analysis. The background set of transcripts used to test our DE set against included all of the transcripts within the transcriptome that mapped significantly to GO terms. Using the 'Biological Networks Gene Ontology' (BiNGO) plugin v. 3.0.3 (Maere *et al.*, 2005) within the Cytoscape software platform v. 3.3.0 (Shannon *et al.*, 2003), I tested for both over- and under-representation using a hypergeometric test at an FDR-adjusted p-value < 0.05.

RESULTS

Each RNA extract produced satisfactory yields, and these were subsequently used in downstream analyses. Total RNA concentration in each sample was generally consistent between NanoDrop and Qubit estimates, the absorbance ratios signified little if any contamination (A260/280 > 2), and the bioanalyzer assay revealed that each sample consisted of high-quality RNA with negligible signs of degradation (RIN > 8; Table 1). The cDNA fragment lengths after library preparation ranged from 80 – 700 bp, with an average of 300 bp. Each sample produced similar numbers of reads, ranging between 28.3 million and 31.1 million. The average quality scores for each base in each sample were ≥ 33 (phred-33 scaling), allowing me to proceed without sequencing error correction. Preprocessing steps led to less than 0.12% of reads being removed in each sample, and the GC content of the samples ranged from 42 – 45% post-trimming.

The *de novo* assembled transcriptome contained a total of 146,023 putative transcript contigs in total, ranging in length from 201–50,751 bp with an average of 1015.83 bp, while the contig N50 of our assembly was 1,998 bp. Approximately 29.62% of the contigs exceeded 1,000 bp in length. Annocript annotated 59,590 (40.80%) contigs with reliable protein annotations from significant (e value < 10^{-5}) BLASTX hits using the UniRef90 database. Of these hits, 96.99% and 93.60% were annotated to insects and lepidopterans, respectively. Mapping GO annotations to these hits resulted in 40,511 transcripts representing 6,476 GO categories in our transcriptome, with 4,075 gene products attributed to biological processes, 815 to cellular components, and 1,586 to molecular function. The top GO terms attributed to the largest numbers of transcript contigs included ‘integral to membrane’ (GO:0016021), ‘nucleic acid

binding' (GO:0003676), 'ATP binding' (GO:0005524), 'nucleus' (GO:0005634), and 'zinc ion binding' (GO:0008270) (Fig. 2).

On average, alignment to this transcriptome produced 47.07% (± 0.25) uniquely mapped reads, 47.04% (± 0.19) multiple-mapping reads, and 1.10% (± 0.02) ambiguously mapped reads (Fig. 3). Based on slight differences in our total read library sizes between samples after quality-filtering, I used TMM normalization resulting in library normalization factors ranging from 0.915–1.104 (± 0.023), which were then multiplied by actual library sizes to find the final effective library sizes (Fig. 4). After filtering out low and no expression transcripts with < 1 CPM, 62,945 out of 146,023 (43.11%) were retained for differential expression analysis.

PCA results indicated strong, non-group-defined clustering of samples along the first two principal axes (Fig. 5; Fig. 6), so I used surrogate variable analysis to remove these batch effects. Two significant surrogate variables which were subsequently included in the negative binomial regression model ascertaining differential expression between the control and exposure groups. Including these surrogate variables as covariates resulted in clear PCA clustering of samples by group (Fig. 7) and improved detection of significant DE transcripts at a FDR < 0.05 (Benjamini and Hochberg, 1995; Storey, 2004) with at least a two-fold change in expression between groups from 75 to 290 transcripts. Heatmap analysis revealed eight clusters of transcripts that displayed similar gene expression changes across our samples (Fig. 8).

Of these 290 transcripts, 136 (47%) had significant BLASTX hits (e-value < 1e-5) with reliable protein annotations, although 24 (8%) of these had uncharacterized functions (Tables 2, 3). The top 11 organisms with the highest number of hits were all also lepidopteran taxa, with most pertaining to *Amyelois transitella* (Lepidoptera: Pyralidae). Of these 136 transcripts with protein annotations, 102 (75%) displayed reliable GO term sequence identity. GO term

enrichment analysis identified 15 overrepresented and 0 underrepresented GO categories in the exposed samples (adjusted p value < 0.05; Table 4). Six of these overrepresented GO terms pertained to glutamate metabolism, biosynthesis, and synthase activity, while dicarboxylic acid biosynthesis and metabolism corresponded to two terms, and oxidoreductase, aminoacylase, FMN binding, chromatin binding, and macromolecular binding were represented by one term each. Notably, 14 out of 15 of these overrepresented GO terms were correlated with a down-regulated set of transcript annotations while only one term pertained to an up-regulated set. Additionally, six terms were related to biological processes while nine terms pertained to molecular function annotations.

Of note is that the majority of transcripts mapping to significantly enriched GO terms occurred as very low or zero transcript count observations in the exposed vs. control groups, as is the case with most of the down-regulated terms. All transcripts mapping to chromatin binding-, glutamate-, integrin-, oxidoreductase-, and aminoacylase-related GO terms exhibited this pattern of "all-or-nothing" transcript expression. As the data included considerable noise, the prevalence of this pattern among the differentially expressed GO annotated transcripts may simply be due to these patterns being the only ones strong enough to discern statistically.

DISCUSSION

The *de novo* transcriptome assembly used here produced 146,023 putative contigs with 54,590 (37.38%) of these having significant BLASTX annotations. This finding is comparable to other *de novo* assemblies performed on brain and other tissues from both invertebrates (McGrath *et al.*, 2016; Roulin *et al.*, 2014; Torkelli *et al.*, 2015) and vertebrates (Deng *et al.*, 2016; Lee *et al.*, 2015; Lin *et al.*, 2016; Salisbury *et al.*, 2015; Sanogo *et al.*, 2011). Salisbury *et al.* (2015) recovered nearly 300,000 *de novo*-assembled unique contigs from brain and central nervous tissue of the ghost knifefish (*Apteronotus leptorhynchus*), while only 42,459 (~14%) of these contigs had significant BLAST annotations, a pattern that mirrors the high number of unique contigs constructed in my assembly with no annotations. Similarly, McGrath *et al.* (2016) constructed a *de novo* transcriptome using brain and central nervous tissue from the lobster *Homarus americanus* with 115,757 contigs while only 34,813 (~30%) of these had significant BLAST annotations. Additionally, these knifefish and lobster transcriptomes exhibited contig N50 measures of 2,539 and 1,289 bp, respectively, which are comparable to our assembly's N50 of 1,998 bp.

The results reported here build on a growing body of literature detailing predator-induced shifts in gene expression in vertebrates and invertebrates (Nanda *et al.*, 2008; Leder *et al.*, 2009). Several studies have focused on describing the gene expression dynamics of large-scale predator-induced morphological changes that occur in organisms displaying predation-related polyphenisms, including multiple species of *Daphnia* (Rozenberg *et al.*, 2015; Schwarzenberger *et al.*, 2009; Spanier *et al.*, 2010) and the Hokkaido salamander (*Hynobius retardatus*; Matsunami *et al.*, 2015). Subtler predator-induced changes also have been studied in diverse taxa, including stickleback fish (Sanogo *et al.*, 2011) and an intertidal snail (Chu *et al.*, 2014).

Exposure to auditory cues of aerial hawking bats for the duration of a single night resulted in significant and strong transcriptomic changes, as measured by absolute transcript fold-changes ranging between 1.2 and 11.5 (log_2), in the brain of *S. frugiperda*. Transcriptomic responses in the brains of repeatedly predator-stressed sticklebacks displayed low-to-moderate fold-change differences, ranging for the most part between 2 and 6 (log_2) (Sanogo *et al.*, 2011), while predator-induced polyphenic *Daphnia* displayed fold-changes ranging from 2 to 10 (log_2) (Rozenberg *et al.*, 2015). Furthermore, the number of DE transcripts found here is comparable to that found in other RNA-seq studies on predator-induced gene expression in invertebrates. For instance, *Daphnia pulex* exposed to kairomones of predatory phantom midge *Chaoborus* larvae displayed 256 DE genes (Rozenberg *et al.*, 2015), while only three transcripts were differentially regulated in the intertidal snail *Nucella lapillus* exposed to seawater that first passed through a chamber holding a predatory crab, *Carcinus maenas,* feeding on *N. lapillus* (Chu *et al.*, 2014). A similar striking difference in the number of DE transcripts from brain tissue after predator exposure has even been reported intraspecifically by Matsunami *et al.* (2015), who found that Hokkaido salamander larvae exposed to predatory dragonfly naiads displayed 605 DE transcripts, while only 103 transcripts were differentially expressed after exposure to predatory tadpoles. Clearly, the degree to which prey respond transcriptionally to predator exposure can vary widely and no clear pattern has yet emerged for these responses in general.

Furthermore, our results indicate a broad range of functional annotations related to our DE transcripts, with up-regulated transcripts coding for proteins that affect cellular signaling pathways, mitochondrial metabolism, oxidoreductase activity, glutamate synthesis, ionotropic chemosensory receptor activity, aminoacylase activity, transcription regulation, ion transport, cilium assembly, and protein, amino acid, and ion binding, as well as others. Each up-regulated

transcript tended to be associated with a single protein or family of protein products, with the exception of two transcripts each related to aminoacylase, ATP-binding, and choline dehydrogenase. Down-regulated transcript annotations also displayed a large degree of functional variability, including endocytosis, cytochrome P450 activity, chromatin-mediated transcription regulation, integrin-mediated signaling pathways, glutamate biosynthesis, voltage-dependent calcium transporter channels, muscle differentiation, and protein transport, among others. Similarly, down-regulated transcripts generally tended to code for an individual protein product, with the notable exceptions of the cytochrome P450 enzymes, integrin proteins, and glutamate synthase.

Several strongly up-regulated transcripts corresponded to unexpected protein annotations, including a mitochondrial calcium uniporter protein (log_2 FC = 9.66), an X-linked retinitis pigmentosa GTPase regulator homolog (log_2 FC = 9.86), mutant cadherin (log_2 FC = 5.60), mitochondrial choline dehydrogenase (log_2 FC = 6.78), and acyl-coenzyme A synthetase short-chain family member 3 (log_2 FC = 6.22). The mitochondrial calcium uniporter protein acts as a transmembrane transporter for uptake of calcium ions into mitochondria (Marchi and Pinton, 2014) after these ions are mobilized from intracellular stores, such as the endoplasmic reticulum, by inositol triphosphate. Notably, another significantly up-regulated transcript among exposed individuals coded for type 2 inositol 1, 4, 5-triphosphate 5-phosphatase (log_2 FC = 6.06). In humans, this phosphatase hydrolyzes inositol triphosphate and functions as a signal-terminating enzyme, preventing intracellular stores from releasing more calcium (Ross *et al.*, 1991). Calcium is utilized by mitochondria for cellular energy production, in balancing cytosolic calcium concentrations, and in determining cell fate by inducing or inhibiting apoptosis, although the role of the up-regulated uniporter is often associated with cellular metabolism (Contreras *et al.*,

2010). Another highly up-regulated transcript corresponded to a mitochondrial acyl coenzyme A synthetase family protein described in humans, which catalyzes the initial reaction in fatty acid metabolism by forming a thioester, usually with acetate (Watkins *et al.*, 2007). Although little can be inferred as to whether this enzyme acts to initiate fatty acid storage or degradation for energy production, my results indicate a strong response of fatty acid metabolism to auditory predator-cue exposure in *S. frugiperda*. Moreover, the up-regulation of mitochondrial choline dehydrogenase, an enzyme localized to the mitochondrial membrane that catalyzes the conversion of choline into betaine aldehyde which is then converted to betaine via betaine aldehyde dehydrogenase (Gadda and McAllister-Wilkins, 2003), suggests that betaine may have been produced at higher levels in the brains of exposed individuals, although the absence of betaine aldehyde dehydrogenase among the DE transcripts remains conspicuous. Betaine is an up-regulator of mitochondrial respiration and exposure to betaine has resulted in increased ATP levels in humans (Lee, 2015). Taking these up-regulated patterns in tandem, I suggest that auditory predator-cue exposure in *S. frugiperda* likely induces increased mitochondrial and cellular metabolism.

The second most up-regulated transcript codes for a X-linked retinitis pigmentosa GTPase regulator (RPGR) homolog, a protein usually associated with cilia development in the photoreceptors of vertebrate eyes (Gakovic *et al.*, 2011), although it localizes to other tissues and cell types as well (Khanna *et al.*, 2005). I suggest that RPGR up-regulation may be related to increased cilia development and neuronal connections but since its expression has not been studied in insect eyes or other tissues, further conclusions about the function of this protein under predator-stressed conditions in *S. frugiperda* cannot be made. Because *S. frugiperda* brains were excised without compromising pigment-storing ommatidial cells, the RPGR expression pattern

observed here likely is intrinsic to brain tissue and may be related to neural tissues extending from innervations of the eye. Notably, the entire suite of phototransducing proteins found in the *Drosophila* visual system is also found to act in the fly's auditory transduction system, with visual rhodopsins serving mechanical transducing and amplifying roles in auditory neurons of the Johnstan's organ (Gopfert and Hennig, 2016).

Another up-regulated transcript that may be related to neuronal development encoded a mutant cadherin protein found in humans. Cadherins are calcium-dependent cell-cell adhesion proteins that are integral in nearly every step of neural development in larval *Drosophila* (Fung *et al.*, 2009), have been implicated in guiding new neuron development contributing to neural plasticity (Edsbagge *et al.*, 2004), and are even involved in hair-bundle development in vertebrate ears (Hirano and Takeichi, 2012). As expression of cadherins is usually repressed and localized only to synaptic areas in mature brain tissues (Hirano and Takeichi, 2012), the fact that it is highly up-regulated in predator-cue exposed *S. frugiperda* coupled with RPGR up-regulation suggests that neural plasticity and development of new neural connections upon exposure to novel environmental cues may play key roles in functionally responding to auditory predator-cues.

Also highly up-regulated ($\log_2$ FC = 7.68) was a transcript annotated as a regulatory-associated protein of target of rapamycin (TOR) complex 1 (RPTOR). RPTOR, an integral component of the TOR complex, functions as a scaffold protein that recruits TOR specific substrates and regulates TOR-induced cellular processes, such as cell growth, survival, and autophagy in response to nutrient stress, hormonal signals, and other stressors (Kwak *et al.*, 2012). A wide-range of environmental stressors induce evolutionarily conserved TOR pathways in taxa ranging from unicellular organisms to vertebrates (Reiling and Sabatini, 2006). Reiling

and Sabatini (2006) argue that TOR's response to nutrient availability, hypoxia, DNA damage, and osmotic stress in vertebrates, along with its responses to osmolarity and temperature in unicellular organisms, suggests that TOR signaling is an ancient mechanism for the surveillance of generalized cellular stress conditions. However, treatment of *Drosophila* with rapamycin induced transcriptional changes in nearly 5% of the all genes in its genome (Guertin *et al.*, 2006), indicating that TOR has a very broad effect on cellular function, making it difficult to conclude that up-regulation of RPTOR is directly related to cellular stress in *S. frugiperda* exposed to predator cues.

Several strongly down-regulated transcripts also mapped to unexpected protein annotations, including a 27 kDa hemolymph protein ($\log_2$ FC = -10.40), DNA N^6-methyladenine demethylase-like isoform X1 (-7.18), decaprenyl-diphosphate synthase subunit 2 ($\log_2$ FC = -6.80), FH1/FH2 domain-containing protein 3 ($\log_2$ FC = -7.85), and protein polybromo-1 (isoform $\log_2$ FC = -9.10, -8.52, -7.60, -7.39, -6.94, 8.54). The 27 kDa hemolymph protein family consists of proteins found in diverse insect taxa but their function remains unknown. One member of this family, however, is annotated in *Manduca sexta* as a glycoprotein precursor (Samaraweera and Law, 1995). Glycoproteins serve multiple functions within insect tissues, and are thought to act in metabolism as energy storage molecules, catalytic enzymes, and protectants for monosaccharides as they are transported through the hemolymph (Rockstein, 1978). Aside from these functions, up-regulation of hemolymph glycoproteins has also been observed in *Locusta migratoria* and *Manduca sexta* after infection with an entomopathogenic fungus (Wang *et al.*, 2007) and parasitism by a braconid wasp (Harwood *et al.*, 1994), respectively. It is possible that down-regulation of this 27 kDa hemolymph protein may signify that hemolymph glycoproteins are less abundant in the brains of predator-cue exposed *S. frugiperda*, yet too little

is known about this family of hemolymph proteins in non-model organisms to draw this conclusion.

DNA N^6-methyladenine (6mA) demethylase is another protein correlated with a highly down-regulated transcript. Methylation of 6mA has been studied primarily in prokaryotes, where it serves as the primary mechanism for epigenetic signaling via DNA methylation — as opposed to the primary mechanism found in eukaryotes, 5-methycytosine (5mC) methylation (Vanyushin *et al.*, 1968). Demethylases associated with 6mA and 5mC serve to remove methyl groups from DNA and RNA, affecting the transcription and translation of affected nucleic acid chains. In plants and vertebrates, 6mA methylation both increases and decreases transcription factor binding (Luo *et al.*, 2015), while in *Drosophila melanogaster* loss of a putative 6mA demethylase resulted in increased transposon expression (Zhang *et al.*, 2015). Notably, a transcript annotated with histone-lysine N-methyltransferase absent, small, or homeotic disc1 (ash1; $\log_2$ FC = -2.54) protein and five transcript isoforms annotated with polybromo-1 (Pb1) protein were down-regulated after predator-cue exposure, although an additional Pb1 isoform was also up-regulated. These two proteins are involved in chromatin remodeling and binding, respectively, wherein ash1 is known to specifically methylate histone H3 Lys-36 (An *et al.*, 2011) while Pb1 interacts with histone H3 during nucleosome assembly (Chandrasekaran and Thompson, 2007). Although the functional significance of the down-regulation of 6mA demethylase, polybromo-1, and ash1 in the brain of predator-exposed *S. frugiperda* is unclear, epigenetic mechanisms appear to be induced in some manner. The epigenetic impact of predator-induced stress remains an area of research deserving of future work.

Decaprenyl-diphosphate synthase subunit 2 (DDSS2) is an enzyme that catalyzes a reaction to supply decaprenyl diphosphate for use in ubiquinone-10 biosynthesis. Ubiquinone-10

is concentrated in mitochondria, where it acts as a component of the electron transport chain during aerobic cellular respiration (Ernster and Dallner, 1995), although it also is found in many diverse organelles at lower concentrations. In this context, ubiquinone-10 acts as an electron transport enzyme moving electrons from enzyme complexes I and II to III in the electron transport chain, a function only it and vitamin K_2 are able to perform (Bhalerao and Clandinin, 2012). Ubiquinone-10 also serves as an antioxidant due to its weak electron affinity when reduced. In this state, electrons are held so loosely that the molecule readily gives up electrons to oxidized substrates. For instance, within mitochondria, ubiquinone-10 prevents the oxidation of DNA nucleotides during interactions between peroxidase and DNA-bound metal ions (Lopez *et al.*, 2010; Miyamae *et al.*, 2013). Although the down-regulation of DDSS2 does not directly imply that lower levels of ubiquinone-10 were present in predator-cue exposed *S. frugiperda*, further studies should examine ubiquinone-10 responses to predator exposure. With knowledge of the increased mitochondrial metabolic activity suggested by several up-regulated transcripts discussed previously, it is surprising that DDSS2 is down-regulated, as a greater need for electron transport substrates and antioxidants with enhanced energy production could be expected. Clearly, there is still much to learn in elucidating the role of DDSS2 in predator-induced stress responses.

Formin homology 1/ formin homology 2 domain-containing protein 3 (FHOD3), another protein that mapped to a highly down-regulated transcript in the predator-exposed *S. frugiperda* brain, acts as an actin regulator with a scaffolding function and has been found, in humans, to affect organogenesis, tissue homeostasis, and cancer-cell invasion (Katoh and Katoh, 2004). Actin, a protein that forms microfilaments and constitutes the actin cytoskeleton in all eukaryotic cells, plays a key role in cellular locomotion and shape (Lodish *et al.*, 2000). FHOD family

proteins are thought to bind to the growing barbed-end of actin polymers and serve both to deliver new actin monomers and promote actin polymerization, effectively mediating the growth of the actin cytoskeleton (Bechtold *et al.*, 2014). FHOD family proteins are regulated by rho-GTPases, a member of which was down-regulated after predator-exposure. Furthermore, actin-binding Lin11, Isl-1, Mec-3 protein 3 and alpha catenin were also down-regulated and act as a scaffold protein (Barrientos *et al.*, 2007) and a cellular linking protein between cadherins and actin-containing filaments (Cooper, 2000; Yamada *et al.*, Drees *et al.*, 2005), respectively. Taking into account that a transcript encoding a mutant cadherin was up-regulated in predator-exposed brains as well, these patterns suggest that the actin cytoskeleton is affected by predator-exposure and that changes in cellular morphology and motility within the brain of *S. frugiperda* may be involved.

I also found evidence that the wingless signaling pathway (Wnt), involved in regulating cell morphology, polarity, cell-cell adhesion, cell motility, cell fate, and cell proliferation through signaling transcriptional changes (Cadigan and Nusse, 1997), has many biochemical components which were mapped reliably to DE transcripts between our control and predator-exposed groups. For instance, casein kinase I gamma-3 (CK1G3) was up-regulated ($\log_2$ FC = 1.38) in exposed individuals and aids in the activation of the Wnt pathway. By phosphorylating low-density lipoprotein receptor-related protein 6 (LRP6), CK1G3 allows axin, another up-regulated protein ($\log_2$ FC = 6.68), to bind to LRP6, a protein that activates the resulting transmembrane signaling cascade (Davidson *et al.*, 2005). The activation of Wnt signaling has been reported to lead to the expression of the c-*myc* proto-oncogene, whose products regulate cell growth and proliferation, as well as nuclear signal transduction and transcription regulation (Ray and Miller, 1991). I also found that a c-*myc* promoter binding protein was down-regulated

($\log_2$ FC = -4.47) after predator exposure, indicating that c-*myc* expression may also be down-regulated, although I found no evidence of differential c-*myc* expression directly. Wnt signaling is fundamental to embryonic and larval development in vertebrates and invertebrates alike, conferring effects on body polarity, cell differentiation, and cell migration (Nusse and Varmus, 1992). More recently, Wnt proteins within neural tissues were found to function in axon guidance (Yoshikawa *et al.*, 2003; Zou, 2004), axon remodeling (Hall *et al.*, 2000), and synaptogenesis (Salinas, 2003), leading to changes in neuronal connections within developing and adult invertebrate and vertebrate nervous systems (Hall *et al.*, 2000). With evidence of differential expression of three separate proteins involved in Wnt signaling within the brains of predator-exposed *S. frugiperda*, I suggest that neuronal re-organization and novel neural connections may be induced upon auditory predator-cue stimulation.

Relative to the list of DE transcript annotations in this study, the overrepresented GO terms enriched in the brains of *S. frugiperda* after predator exposure were largely restricted to three main biochemical pathways: 1) chromatin and macromolecule binding, 2) glutamate synthesis and metabolism, and 3) aminoacylase activity, although terms related to oxidoreductase activity, flavin mononucleotide (FMN) binding, and integrin-mediated signaling also were overrepresented. To the best of my knowledge, these GO terms have not been implicated in any other study of predator-induced transcriptional responses, even those pertaining specifically to neural and brain tissues, suggesting that these also represent novel predation-cue induced processes. The small set of GO-annotated DE transcripts identified here limit the statistical detection of subtly over- and under-represented terms; regardless, I found 15 GO terms to be highly significantly overrepresented in our set of annotated DE transcripts relative to the frequency at which these terms were found in our GO-annotated transcriptome (p

< 0.0004). Chromatin binding ($p < 0.0000$) and macromolecular complex binding ($p < 0.0000$) were the most highly overrepresented GO terms identified both with 7 out of 102 GO-annotated DE transcripts mapped to these terms. The binding of cellular proteins to chromatin can elicit varied cellular responses, such as transcriptional regulation, DNA replication, and chromatin remodeling (Ricke and Bielinsky, 2005). Taking into account that transcripts mapping to ash1 and Pb1 protein annotations were also differentially regulated, the presence of these GO terms again implies that epigenetic modifications seem to be induced upon exposure to predator cues.

The set of GO terms pertaining to glutamate synthesis and metabolism included glutamate synthase activity, as well as glutamate biosynthesis and metabolism, glutamine family amino acid biosynthesis, and dicarboxylic acid biosynthesis and metabolism. Glutamate, an amino acid anion derived from its dicarboxylic state, glutamic acid, is used during protein synthesis (Plimmer, 1912), but it also is considered the most abundant excitatory neurotransmitter in the vertebrate brain (Locatelli *et al.*, 2005). Although acetylcholine is the primary excitatory neurotransmitter in the insect nervous system (Wnuk *et al.*, 2014), glutamate also plays an excitatory role (Leboulle *et al.*, 2012) as glutamate immunoreactivity (Sinakevitch *et al.*, 2001) and glutamate-induced ion currents (Cayre *et al.*, 1999) have been reported in insect neurons. Intriguingly, application of glutamate to the mushroom body brain regions of the honeybee, *Apis mellifera*, facilitates glutamatergic neurotransmission and olfactory learning (Locatelli *et al.*, 2005), and glutamate-mediated neurotransmission has also been implicated in the visual (Liang *et al.*, 2012) and tactile (Bernadou *et al.*, 2009) sensory systems. Notably, one of the strongly up-regulated ($\log_2$ FC = 5.70) transcripts I found mapped to a fragment of the ionotropic receptor 75d (IR75d) putative chemosensory protein found in *Spodoptera littoralis*. IR75d is a recently described protein related to ionotropic glutamate receptors (iGluRs), a

conserved family of synaptic glutamate-gated ion channels involved in neuronal communication, and was discovered in the *Drosophila melanogaster* genome by BLAST comparisons of six antennal-expressed olfactory sensing proteins (Benton *et al.*, 2009). Benton *et al.* (2009) found that IR75d and 69 other novel IR-family proteins retained iGluR-like amino acid positions and surmised that IRs may form ion-gated channels and act in chemosensory neuronal signaling, much like iGluRs (Mayer, 2006). Although 21 of these 69 novel IRs showed transcriptional responses to chemical signals in the *Drosophila* antenna, including IR75d, the remaining 46 showed no chemosensory-induced expression (Benton *et al.*, 2009). Knowing that biochemical pathways pertaining to glutamate production were altered in the brains of predator-cue exposed *S. frugiperda* coupled with evidence that IR75d was up-regulated post-exposure, I suggest that IR75d and its relatives may be involved in neuronal communication upon stimulation by non-chemical sensory signals. Further work investigating the expression of IR75d and its family members in response to varied sensory stimuli, particularly in neurons within the *Drosophila* chordotonal Johnston's organ, could lead to insights into the functional significance of previously characterized and uncharacterized IR proteins.

These broad predator-induced transcriptional responses are characteristic of those found in previous studies, such as in predator-stressed stickleback fish (Sanogo *et al.*, 2011), *Daphnia* (Rozenberg *et al.*, 2015), and the Hokkaido salamander (Matsunami *et al.*, 2015). Contrary to our expectations, there is little overlap between previously reported responses to predator-induced stress, such as neuropeptide production and increased antioxidant activity, and the novel predator-induced functional annotations reported here. However, mitoferrin, a solute carrier responsible for iron uptake by red blood cells in vertebrates, was significantly up-regulated in the brains of stickleback fish repeatedly exposed to a chemical predator-cue (Sanogo *et al.*, 2011),

although it was down-regulated (log_2 FC = -6.06) in *S. frugiperda* post-exposure. In insects, the function of mitoferrin is less well understood; *D. melanogaster* with mitoferrin mutations experienced problems with spermatogenesis and development to adulthood (Metzendorf, 2010). Apart from this similarity, the novel transcriptional responses to predation in *S. frugiperda* observed here may be specialized to auditory reception or perhaps found only in Lepidoptera. Furthermore, although efforts were made to avoid auditory habituation to the bat calls in this study, the expression profiles described here bear similarities to past studies of bird-song habituation in the brains of zebra finches (*Taeniopygia guttata*), with both resulting in the downregulation of gene products pertaining to cytoskeletal function and mitochondrial metabolism (Dong *et al.*, 2009). Further work, such as comparing expression profiles through time and between very frequent and infrequent cue exposure regimes would likely aid in parsing the effects due to habituation and those actually induced by predator-cue exposure.

Along with evidence suggesting that physiological and behavioral predator-induced stress responses (Bell *et al.*, 2010; Beleznai *et al.*, 2015) as well as gene expression patterns (Rey *et al.*, 2013) vary between intraspecific individuals, investigating the transcriptional dynamics of individualized stress responses may be an informative line of future research that could help describe the variability of predator-induced transcriptional responses, even within a single prey species. Further transcriptomic inferences would be significantly bolstered with access to an annotated *S. frugiperda* reference genome, which would likely help resolve the identity of the many DE transcripts found here that presently have no reliable protein annotations or uncharacterized functions. As synergistic effects of predator-cue exposure and other unintended stimuli, such as temperature fluctuations between the rearing chamber and sound chamber and light exposure immediately preceding the placement of *S. frugiperda* in the darkened sound

chambers, may lead to transcriptional responses that would not have been observed if the stimuli were isolated (Altshuler *et al.*, 2015), future investigations of auditory predator-cues on transcription in prey organisms should be rigorously designed so as to avoid confounding stimuli.

This study has demonstrated that exposure to ecologically relevant auditory cues of predation risk in *S. frugiperda* results in varied but strong patterns of up- and down-regulation of a broad range of protein products within the moth brain. The most strongly up- and down-regulated transcripts found in this study correspond to many cellular functions which include mitochondrial metabolism, glutamate synthesis and metabolism, actin cytoskeleton morphology, cellular locomotion, axon guidance, restructuring of neural connections, and epigenetic modifications, such as chromatin remodeling and demethylation. This is a promising first step in developing a model for the transcriptional impacts of frequent and repeated exposure to bat predation cues in *S. frugiperda*, which may represent acute and chronic responses of cells to predator-induced stress. Several novel predator-cue induced transcriptional pathways are implicated in these results and present promising opportunities for future research. Specifically, quantitative reverse-transcriptase polymerase chain reaction (RT-qPCR) could be used to validate the presence of gene products and mRNA expression levels observed via RNA-Seq, at least for the transcripts with the highest fold-change differences. Additionally, producing a detailed time-course transcriptional profile beginning after the first moments of predator-cue exposure and concluding after exposure for the entire adult life of *S. frugiperda* would provide insights into the temporal dynamics of the mRNA transcripts identified in this study throughout acute and prolonged cellular responses.

Building on these descriptive studies of predator-cue induced transcriptional dynamics, potential applications abound for enhancing the effectiveness of predation-related biocontrol techniques on managing nocturnal flying pest insect populations. With evidence that bat predation can be up to three times more effective in mitigating insect-related herbivory compared to bird predation (Kalka *et al.*, 2008), the value of bats for biocontrol-based pest management is clear. Investigating whether exposure to predation-related cues, such as ultrasonic bat calls, inhibits insect herbivory on a community level is a next step toward the development of effective, sustainable biocontrol approaches. For instance, the application of predator cues, such as recorded bat calls and bird song, or the recruitment of dense predator populations may be found to influence the distribution, behavior, and physiology of insect pests, aside from their direct impacts on pest mortality. Furthermore, novel genetic approaches to managing pest insect populations have emerged, including RNA interference (RNAi; Zhang *et al.*, 2013; Shah *et al.*, 2014; Ulrich *et al.*, 2015). The use of RNAi-induced gene silencing for insect pest management is limited by the need to identify effective target genes for manipulation and the efficient delivery of gene-modifying agents to target organisms (Zhang *et al.*, 2013). As these challenges are surmounted, investigating the impact of silencing genes integral to the auditory recognition of predator cues and subsequent behavioral and physiological responses, perhaps using this study to identify potential target genes, could lead to the development of genetic modifications that may enhance natural predation-related biocontrol methods.

REFERENCES

Adamo, S.A., Kovalko, I. and Mosher, B. (2013). The behavioral effects of predator-induced stress responses in the cricket (*Gryllus texensis*): the upside of the stress response. *The Journal of Experimental Biology*, 216, 4608–4614.

Altshuler, I., McLeod, A. M., Colbourne, J. K., Yan, N. D. and Cristescu, M. E. (2015). Synergistic interactions of biotic and abiotic environmental stressors on gene expression. *Genome*, 58, 99–109.

An, S., Yeo, K. J., Yeon, Y. H. and Song, J. J. (2011). Crystal structure of the human histone methyltransferase ASH1L catalytic domain and its implications for the regulatory mechanism. *Journal of Biological Chemistry*, 286(10), 6369–8374.

Andrews, S. (2010). FastQC: a quality control tool for high throughput sequence data. Available online at: http://www.bioinformatics.babraham.ac.uk/projects/fastqc

Aruda, A. M., Baumgartner, M. F., Reitzel, A. M. and Tarrant, A. M. (2011). Heat shock protein expression during stress and diapause in the marine copepod *Calanus finmarchicus*. *Journal of Insect Physiology*, 57, 665–675.

Arun, C.P. (2004). Fight of flight, forbearance and fortitude: the spectrum of actions of the catecholamines and their cousins. *Annals of the New York Academy of Sciences*, 1018, 137–140.

Barks, P. M. and Godin, J. J. (2013). Can convict cichlids (*Amatitlania siquia*) socially learn the degree of predation risk associated with the novel visual cues in their environment? *PLoS ONE*, 8(9), 1.

Barrientos, T., Frank, D., Kuwahara, K., Bezprozvannaya, S., Pipes, G. C., Bassel-Duby, R., Richardson, J. A., Katus, H. A., Olsen, E. N. and Frey, N. (2007). Two novel members of

the ABLIM protein family, ABLIM-2 and -3, associate with STARS and directly bind F-actin. *Journal of Biological Chemistry*, 282(11), 8393–8403.

Bechtold, M., Schultz, J. and Bogdan, S. (2014). FHOD proteins in actin dynamics—a formin' class of its own. *Small GTPases*, 5(2), 1–6.

Beckerman, A. P., Wieski, K. and Baird, D. J. (2007). Behavioural versus physiological mediation of life history under predation risk. *Oecologia*, 152, 335–343.

Beleznai, O., Tholt, G., Toth, Z., Horvath, V., Marczali, Z. and Samu, F. (2015). Cool headed individual are better survivors: non-consumptive and consumptive effects of a generalist predator on a sap feeding insect. *PLoS ONE*, 10(8), e0135954, doi.:10.1371/journal.pone.0135954.

Bell, A. M., Henderson, L. and Huntingford, F. A. (2010). Behavioral and respiratory responses to stressors in multiple populations of three-spined sticklebacks that differ in predation pressure. *Journal of Comparative Physiology B*, 180, 211–220.

Benjamini, Y. and Hochberg, Y. (1995). Controlling the false discovery rate: a practical and powerful approach to multiple testing. *Journal of the Royal Statistical Society B*, 57, 289–300.

Benton, R., Vannice, K. S., Gomez-Diaz, C. and Vosshall, L. B. (2009). Variant ionotropic glutamate receptors as chemosensory receptors in *Drosophila*. *Cell*, 136(1), 149–162.

Bhalerao, S. and Clandinin, T. R. (2012). Vitamin K_2 Takes Charge. *Science*, 336(6086), 1241–1242.

Bolger, A. M., Lohse, M. and Usadel, B. (2014). Trimmomatic: A flexible trimmer for Illumina Sequence Data. *Bioinformatics*, btu170.

Boyan, G. S. and Fullard, J. H. (1986). Interneurones responding to sound in the tobacco budworm moth *Heliothis viriscens* (Noctuidae): morphological and physiological characteristics. *Journal of Comparative Physiology A*, 158, 391–404.

Breviglieri, C., Piccoli, G., Uieda, W. and Romero, G. (2013). Predation-risk effects of predator identity on the foraging behaviors of frugivorous bats. *Oecologia*, 173(3), 905–912.

Brown, J.S., Laundre, J. W. and Gurung, M. (1999). The ecology of fear: optimal foraging, game theory, and trophic interactions. *Journal of Mammalogy*, 80(2), 385–399.

Cadigan, K. M. and Nusse, R. (1997). Wnt signaling: a common theme in animal development. *Genes & Development*, 11(24), 3286–3305.

Camacho, C., Coulouris, G., Avagyan, V., Ma, N., Papadopoulos, J., Bealer, K. and Madden, T. L. (2009). BLAST+: architecture and applications. *BMC Bioinformatics*, 10, 421.

Cannon, W. B. (1915). *Bodily Changes In Pain, Hunger, Fear And Rage.* D. Appleton and Company, New York, NY.

Cantor, C. (2009). Post-traumatic stress disorder: evolutionary perspectives. *Australian and New Zealand Journal of Psychiatry*, 43, 1038-1048.

Cayre, M., Buckingham, S. D., Yagodin, S., Sattelle, D. B. (1999). Cultured insect mushroom body neurons express functional receptors for acetylcholine, GABA, glutamate, octopamine, and dopamine. *Journal of Neurophysiology*, 81, 1–14.

Chandrasekaran, R. and Thompson, M. (2007). Polybromo-1-bromodomains bind histone H3 at specific acetyl-lysine positions. *Biochemical and Biophysical Research Communications*, 355(3), 661–666.

Chang, Z., G. Li, J. Liu, Y. Zhang, C. Ashby, D. Liu, C.L. Cramer, and X. Huang. (2015). Bridger: a new framework for *de novo* transcriptome assembly using RNA-seq data. *Genome Biology,* 16, 30. DOI: 10.1186/s13059-015-0596-2.

Chen, Y-L., Hung, Y-S. and Yang, E-C. (2008). Biogenic amine levels change in the brains of stressed honeybees. *Archives of Insect Biochemistry and Physiology*, 68, 241–250.

Chu, N. D., Miller, L. P., Kaluziak, S. T., Trussell, G. C. and Vollmer, S. T. (2014). Thermal stress and predation risk trigger distinct transcriptomic responses in the intertidal snail *Nucella lapillus*. *Molecular Ecology*, 23, 6104-6113.

Clinchy, M., Sheriff, M. J. and Zanette, L. Y. (2013). Predator-induced stress and the ecology of fear. *Functional Ecology* 27(1), 56–65.

Clinchy, M., Zanette, L., Boonstra, R., Wingfield, J. C. and Smith, J. N. M. (2004). Balancing food and predator pressure induces chronic stress in songbirds. *Proceedings of the Royal Society B: Biological Sciences*, 271, 2473–2479.

Conner, W.E. and Corcoran, A. J. (2012). Sound strategies: the 65-million-year-old battle between bats and insects. *Annual Review of Entomology*, 57, 21–39.

Contreras, L., Drago, I., Zampese, E. and Pozzan, T. (2010). Mitochondria: The calcium connection. *Biochimica et Biophysica Acta (BBA) – Bioenergetics*, 1797(6–7), 607–618.

Cooke, S. J., Steinmetz, J., Degner, J. F., Grant, E. C., and Philipp, D. P. (2003). Metabolic fright responses of different-sized largemouth bass (*Micropterus salmoides*) to two avian predators show variations in nonlethal energetic costs. *Canadian Journal of Zoology*, 81, 699–709.

Cooper, G. M. (2000). *The Cell: A Molecular Approach*. Sunderland, MA, USA: Sinauer Associates.

Creel, S. and Christianson, D. (2008). Relationships between direct predation and risk effects. *Trends in Ecology and Evolution*, 23, 194–201.

Davidson, G., Wu, W., Shen, J., Bilic, J., Fenger, U., Stannek, P., Glinka, A. and Niehrs, C. (2005). Casein kinase 1 γ couples Wnt receptor activation to cytoplasmic signal transduction. *Nature*, 438(7069), 867–872.

Deng, T., Pang, C., Lu, X., Zhu, P., Duan, A., Tan, Zhengzhun, Huang, J., Li, H., Chen, M. and Liang, X. (2016). *De novo* transcriptome assembly of the chinese swamp buffalo by rna sequencing and ssr marker discovery. *PLoS ONE*, 11(1), e0147132.

Dobin, A., Davis, C. A., Schlesinger, F., Drenkow, J., Zaleski, C., Jha, S., Batut, P., Chaisson, M. and Gingeras, T. R. (2013). STAR: ultrafast universal RNA-seq aligner. *Bioinformatics*, 29(1), 15–21.

Dong, S., Replogle, K. L., Hasadsri, L, Imai, B. S., Yau, P. M., Rodriguez-Zas, S., Southey, B. R., Sweedler, J. V. and Clayton, D. F. (2009). Discrete molecular states in the brain accompany changing responses to a vocal signal. *Proceedings of the National Academy of Sciences*, 106(27), 11364–11369.

Drees, F., Pokutta, S., Yamada, S., Nelson, W. J. and Weis, W. I. (2005). α-catenin is a molecular switch that binds e-cadherin-β-catenin and regulates actin-filament assembly. *Cell*, 123(5), 903–915.

Edsbagge, J., Zhu, S., Xiao, M. Y., Wigstrom, H., Mohammed, A. H. and Semb, H. (2004). Expression of dominant negative cadherin in the adult mouse brain modifies rearing behavior. *Molecular and Cellular Neuroscience*, 25(3), 524–535.

Eilam, D., Dayan, T., Ben-Eliyahu, S., Schulman, I., Shefer, G. and Hendrie, C. A. (1999). Differential behavioural and hormonal responses of voles and spiny mice to owl calls.

Animal Behaviour, 58, 1085–1093.

Elvira, S., Gorria, N., Munoz, D., Williams, T. and Caballero, P. (2010). A simplified low-cost diet for rearing *Spodoptera exigua* (Lepdioptera: Noctuidae) and its effect on *S. exigua* nucleopolyhedrovirus production. *Journal of Economic Entomology*, 103(1), 17–24.

Ernster, L. and Dallner, G. (1995). Biochemical, physiological, and medica aspects of ubiquinone function. *Biochemica et Biophysica Acta*, 1271(1), 195–204.

Even, N., Devaud, J-M. and Barron, A. B. (2012). General stress responses in the honey bee. *Insects*, 3, 1271–1298.

Fleshner, M., Campisi, J., Amiri, L., and Diamond, D.M. (2004). Cat exposure induces both intra- and extracellular Hsp72: the roles of adrenal hormones. *Psychoneuroendocrinology* 29, 1142–1152.

Fullard, J. H. (1988). The tuning of moth ears. *Experientia*, 44, 423–428.

Fullard, J. H., Dawson, J. W. and Jacobs, D. S. (2003). Auditory encoding during the last moment of a moth's life. *The Journal of Experimental Biology*, 206, 281–294.

Fung, S., Wang, F., Spindler, S. R. and Hartenstein, V. (2009). *Drosophila* E-cadherin and its binding partner Armadillo/ β-catenin are required for axonal pathway choices in the developing larval brain. *Developmental Biology*, 332(2), 371–382.

Gadda, G. and McAllister-Wilkins, E. E. (2003). Cloning, expression, and purification of choline dehydrogenase from the moderate halophile *Halomonas elongata*. *Applied Environmental Microbiology*, 69(4), 2126–2132.

Gäde, G., Marco, H. G., Simek, P., Audsley, N., Clark, K. D. and Weaver, R.J. (2008). Predicted versus expressed adipokinetic hormones, and other small peptides from the corpus

cardiacum-corpus allatum: A case study with beetles and moths. *Peptides*, 29, 1124–1139.

Gakovic, M., Shu, X., Kasioulis, I., Carpanini, S., Moraga, I. and Wright, A. F. (2011). The role of RPGR in cilia formation and actin stability. *Human Molecular Genetics*, 20(24), 4840–4850.

Gopfert, M. C. and Hennig, R. M. (2016). Hearing in insects. *Annual Review of Entomology*, 61, 257–276.

Grabherr, M. G., Haas, B. J., Yassour, M., Levin, J. Z., Thompson, D. A., Amit, I., Adiconis, X., Fan, L., Raychowdhury, R., Zeng, Q., Chen, Z., Mauceli, E., Hacohen, N., Gnirke, A., Rhind, N., di Palma, F., Birren, B. W., Nusbaum, C., Lindblad-Toh, K., Friedman, N. and Regev, A. (2011). Full-length transcriptome assembly from RNA-seq data without a reference genome. *Nature Biotechnology*, 29(7), 644–652. doi: 10.1038/nbt.1883.

Greenfield, M. D., Tourtellot, M. K., Tillberg, C., Bell, W. J. and Prins, N. (2002). Acoustic orientation via sequential comparison in an ultrasonic moth. *Naturwiss*, 89(8): 376–380.

Guertin, D. A., Guntur, K. V., Bell, G. W., Thoreen, C. C. and Sabatini, D. M. (2006). Functional genomics identifies TOR-regulated genes that control growth and division. *Current Biology*, 16(10), 958–970.

Haas, B. J., Papanicolaou, A., Yassour, M., Grabherr, M., Blood, P. D., Bowden, J., Couger, M. B., Eccles, D., Li, B., Lieber, M., MacManes, M. D., Ott, M., Orvis, J., Pochet, N., Strozzi, F., Weeks, N., Westerman, R., William, T., Dewey, C. N., Henschel, R., LeDuc, R. D., Friedman, N., and Regev, A. (2013). *De novo* transcript sequence reconstruction from RNA-seq using Trinity platform for reference generation and analysis. *Nature Protocols*, 8, 1494–1512.

Hall, A. C., Lucas, F. R. and Salinas, P. C. (2000). Axonal remodeling and synaptic differentiation in the cerebellum is regulated by WNT-7a signaling. *Cell*, 100, 525–535.

Harwood, S. H., Grosovsky, A. J., Cowles, E. A., Davis, J. W. and Beckage, N. E. (1994). An abundantly expressed hemolymph glycoprotein isolated from newly parasitized *Manduca sexta* larvae is a polydnavirus gene product. *Virology*, 205(2), 381–392.

Hawlena, D., Kress, H., Dufresne, E. R. and Schmitz, O. J. (2011). Grasshoppers alter jumping biomechanics to enhance escape performance under chronic risk of spider predation. *Functional Ecology*, 25(1), 279–288.

Hawlena, D. and Schmitz, O. J. (2010). Physiological stress as a fundamental mechanism linking predation to ecosystem functioning. *The American Naturalist*, 176, 537–556.

Hedwig, B. G. (2016). Sequential filtering processes shape feature detection in crickets: a framework for song pattern recognition. *Frontiers in Physiology*, 7, 46.

Hirano, S. and Takeichi, M. (2012). Cadherins and Brain Morphogenesis and Wiring. *Physiological Reviews*, 92(2), 597–634.

Hubbs, A. H., J. S. Millar, and J. P. Wiebe. 2000. Effect of brief exposure to a potential predator on cortisol concentrations in female Columbian ground squirrels (*Spermophilus columbianus*). *Canadian Journal of Zoology*, 78, 578–587.

Jung, K., Kalko, E. K. V., and von Helversen, O. (2007). Echolocation calls in Central American emballonurid bats: signal design and call frequency alternation. *Journal of Zoology*, 272, 125–137.

Kagawa, N., Ryo, K., and Mugiya, Y. (1999). Enhanced expression of stress protein 70 in the brains of goldfish, *Carassius auratus*, reared with bluegills, *Lepomis macrochirus*. *Fish Physiology and Biochemistry*, 21, 103–110.

Kalka, M. B., Smith, A. R. and Kalko, E. K. V. (2008). Bats limit arthropods and herbivory in a tropical forest. *Science*, 320(5872), 71.

Katoh, M. and Katoh, M. (2004). Identification and characterization of human FHOD3 gene *in silico*. *International Journal of Molecular Medicine*, 13(4), 615–620.

Khanna, H., Hurd, T. W., Lillo, C., Shu, X., Parapuram, S. K., He, S., Akimoto, M., Wright, A. F., Margolis, B., Williams, D. S. and Swaroop, A. (2005). RPGR-ORF15, which is mutated in retinitis pigmentosa, associates with smc1, smc3, and microtubule transport proteins. *Journal of Biological Chemistry*, 280(39), 33580–33587.

Krebs, C. J. (2002). Two complementary paradigms for analyzing population dynamics. *Philosophical Transactions of the Royal Society of London. B, Biological Sciences*, 257, 1211–1219.

Krebs, C. J., Boutin, S., Boonstra, R., Sinclair, A. R. E., Smith, J. N. M., Dale, M. R. T., Martin, K. and Turkington, R. (1995). Impact of food and predation on the snowshoe hare cycle. *Science*, 269, 1112–1115.

Kwak, D., Choi, S., Jeong, H., Jang, J-H., Lee, Y., Jeon, H., Lee, M. N., Noh, J., Cho, K., Yoo, J. S., Hwang, D., Suh, P-G. and Ryu, S. H. (2012). Osmotic stress regulates mammalian target of rapamycin (mTOR) complex 1 via c-jun N-terminal kinase (JNK)-mediated raptor protein phosphorylation. *The Journal of Biological Chemistry*, 287, 18398–18407.

Langfelder, P., Zhang, B. and Horvath, S. (2008). Defining clusters from a hierarchical cluster tree: the Dynamic Tree Cut package for R. *Bioinformatics*, 24(5), 719–720.

Law, C. W., Chen, Y., Shi, W. and Smyth, G. K. (2014). Voom: precision weights unlock linear model analysis tools for RNA-seq read counts. *Genome Biology*, 15, R29.

Leboulle, G. (2012). Glutamate neurotransmission in the honey bee central nervous system. In *Honeybee Neurobiology and Behavior: A Tribute to Randolf Menzel* (ed. C. G. Galizia, D. Eisenhardt, and M. Giurfa), pp. 171–184. Heidelburg, Germany: Springer Science + Business Media.

Leder, E. H., Merila, J. and Primmer, C. R. (2009). A flexible whole-genome microarray for transcriptomics in three-spine stickleback (*Gasterosteus aculeatus*). *BMC Genomics*, 10, 426.

Lee, A. K., Kulscar, K. A., Elliott, O., Khiabanian, H., Nagle, E. R., Jones, M. E. B., Amman, B. R., Sanchez-Lockhart, M., Towner, J. S., Palacios, G. and Rabadan, R. (2015). De novo transcriptome reconstruction and annotation of the Egyptian rousette bat. *BMC Genomics*, 16, 1033.

Lee, I. (2015). Betaine is a positive regulator of mitochondrial respiration. *Biochemical and Biophysical Research Communications*, 456(2), 621-625.

Leek, J., Johnson, W. E., Jaffe, A., Parker, H. and Storey, J. (2015). The SVA package for removing batch effects and other unwanted variation in high-throughput experiments. R package version 3.18.

Leek, J., Scharpf, R. B., Bravo, H. C., Simcha, D., Langmead, B., Johnson, W. E., Geman, D., Baggerly, K. and Irizarry, R. A. (2010). Tackling the widespread and critical impact of batch effects in high-throughput data. *Nature Review Genetics*, 11, 733–739.

Liang, Z. S., Nguyen, T., Mattila, H. R., Rodriguez-Zas, S. L., Seeley, T. D. and Robinson, G. E. (2012). Molecular determinants of scouting behavior in honey bees. *Science*, 335, 1225–1228.

Lin, Q., Luo W., Wan, S. and Gao, Z. (2016). *De novo* transcriptome analysis of two seahorse species (*Hippocampus erectus* and *H. mohnikei*) and the development of molecular markers for population genetics. *PLoS ONE*, 11(4), e0154096. doi:10.1371/journal.pone.0154096.

Locatelli, F. Bundrock, G. and Muller, U. (2005). Focal and temporal release of glutamate in the mushroom bodies improves olfactory memory in *apis mellifera*. *The Journal of Neuroscience*, 25(50), 11614–11618.

Lodish, H., Berk, A., Zipursky, S. L., Matsudaira, P., Baltimore, D. and Darnell, J. (2000). *Molecular Cell Biology. 4th Edition*. New York, NY: W. H. Freeman & Company.

Lopez, L. C., Quinzii, C. M., Area, E., Naini, A. Rahman, S., Schuelke, M., Salvati, L., DiMauro, S. and Hirano, M. (2010). Treatment of CoQ_{10} deficient fibroblasts with ubiquinone, coq analogs, and vitamin c: time- and compound-dependent effects. *PLoS ONE*, 5(7), e11897. doi:10.1371/journal.pone.0011897.

Luo, G-Z., Blanco, M. A., Greer, E. L., He, C. and Shi, Y. (2015). DNA N^6-methyladenine: a new epigenetic mark in eukaryotes? *Nature Reviews Molecular Cell Biology*, 16, 705–710.

MacDonald JW (2008). affycoretools: Functions useful for those doing repetitive analyses with Affymetrix GeneChips. R package version 1.42.0.

Maere, S., Heymans, K. and Kuiper, M. (2005). BiNGO: a Cytoscape plugin to assess overrepresentation of Gene Ontology categories in biological networks. *Bioinformatics*, 21, 3448–3449.

Marchi, S. and Pinton, P. (2014). The mitochondrial calcium uniporter complex: molecular components, structure and physiopathological implications. *The Journal of Physiology*, 595(5), 829–839.

Matsunami, M., Kitano, J., Kishida, O., Michimae, H., Miura, T. and Nishimura, K. (2015). Transcriptome analysis of predator- and prey-induced phenotypic plasticity in the Hokkaido salamander (*Hynobius retardatus*). *Molecular Ecology* 3064-3076.

McNeil, J. and Acharya, L. (1998). Predation risk and mating behavior: the responses of moths to bat-like ultrasound. *Behavioral Ecology*, 9(6), 552–558.

McGrath, L. L., Vollmer, S. V, Kaluziak, S. T. and Ayers, J. (2016). *De novo* transcriptome assembly for the lobster *Homarus americanus* and characterization of differential gene expression across nervous system tissues. *BMC Genomics*, 17, 63.

Mella, V. S. A., Banks, P. B. and McArthur, C. (2014). Negotiating multiple cues of predation risk in a landscape of fear: what scares free-ranging brushtail possums? *Journal of Zoology*, 294(1), 22–30.

Metzendorf, C. (2010). Mitochondrial iron metabolism. Study of mitoferrin in *Drosophila melanogaster*. *Digital Comprehensive Summaries of Uppsala Dissertations from the Faculty of Science and Technology*, 713, 1–55.

Miller, J. R. B., Ament, J. M. and Schmitz, O. J. (2014). Fear on the move: predator hunting mode predicts variation in prey mortality and plasticity in prey spatial response. *Journal of Animal Ecology*, 83(1), 214–222.

Miller, L. A. and Surlykke, A. (2001). How some insects detect and avoid being eaten by bats: tactics and countertactics of prey and predator. *BioScience*, 51(7), 570–581.

Miyamae, T. Seki, M., Naga, T., Uchino, S., Asazuma, H., Yoshida, T., Iizuka, Y., Kikuchi, M., Imagawa, T., Natsumeda, Y., Yokota, S. and Yamamoto Y. (2013). Increased oxidative stress and coenzyme Q10 deficiency in juvenile fibromyalgia: amelioration of hypercholesterolemia and fatigue by ubiquinol-10 supplementation. *Redox Report*, 18(1), 12–19.

Monclus, R., Palomares, F., Tablado, Z., Martinez-Fonturbel, A. and Palme, R. (2009). Testing the threat-sensitive predator avoidance hypothesis: physiological responses and predator pressure in wild rabbits. *Oecologia*, 158, 615–623.

Mora, E. C., Macias, S., Vater, M., Coro, F. and Kossl, M. (2004). Specializations for aerial hawking in the echolocation system of *Molossus molossus* (Molossidae, Chiroptera). *Journal of Comparative Physiology A*, 190, 561–574.

Mullner, D. (2013). Fastcluster: fast hierarchical, agglomerative clustering routines for R and Python. *Journal of Statistical Software*, 53(9), 1–18.

Musacchia, F., Basu, S., Petrosino, G., Salvermini, M. and Sangers, R. (2015). Annocript: a flexible pipeline for the annotation of transcriptomes able to identify putative long noncoding RNAs. *Bioinformatics*, 31(13), 2199–2201.

Nanda, S. A., Qi, C., Roseboom, P. H. and Kalin, N. H. (2008). Predator stress induces behavioral inhibition and amygdala somatostatin receptor 2 gene expression. *Genes, Brain and Behavior*, 7, 639-648.

Norman, A. P. and Jones, G. (2000). Size, peripheral auditory tuning and target strength in noctuid moths. *Physiological Entomology*, 25, 346–353.

Nusse, R. and Varmus, H. E. (1992). Wnt genes. *Cell*, 69(7), 1073–1087.

Olberg, R. M. and Willis, M. A. (1990). Pheromone-modulated optometer response in male gypsy moths *Lymantria dispar* L.: Directionally selective visual interneurons in the ventral nerve cord. *Journal of Comparative Physiology A*, 167, 707–714.

Organ, C. L., Moreno, R. G. and Edwards, S. V. (2008). Three tiers of genome evolution in reptiles. *Integrative and Comparative Biology*, 48(4), 494–504.

Patro, R., Duggal, G. and Kingsford, C. (2015). Accurate, fast, and model-aware transcript expression quantification with Salmon. *bioRxiv.org*, doi: http://dx.doi.org/10.1101/021592.

Pauwels, K., Stoks, R., and De Meester, L. (2005). Coping with predator stress: interclonal differences in induction of heat-shock proteins in the water flea Daphnia magna. *Journal of Evolutionary Biology*, 18, 867–872.

Peric-Mataruga, V., Nenadovic, V. and Ivanovic, J. (2006). Neurohormones in insect stress: a review. *Archives of Biological Science Belgrade*, 58(1), 1–12

Peckarsky, B. L., Cowan, C. A., Penton, M. A. and Anderson, C. (1993). Sublethal consequences of stream-dwelling predatory stoneflies on mayfly growth and fecundity. *Ecology*, 74, 1836–1846.

Pfuhl, G., Kalinova, B., Valterova, I. and Berg, B. G. (2015). Simple ears – flexible behavior:

Information processing in the moth auditory pathway. 61(2), 292–302.

Pfuhl, G., Zhao, X. C., Surlykke, A. and Berg, B. G. (2014). Sound-responding neurons innervate the ventro-lateral protocerebrum of the heliothine moth brain. *Cell Tissue Research*, 355, 289–302.

Plimmer, R. H. A. (1912). The chemical constitution of the protein. In *Monographs on Biochemistry. Part I. Analysis (2nd Edition)*, (ed. R. H. A. Plimmer and F. G. Hopkins), pp. 114. London, UK: Longmans, Green and Co.

Polednik, L., Rehulka, J., Kranz, A., Polednikova, K., Hlavac, V. and Kazihnitkova, H. (2008). Physiological responses of over-wintering common carp (*Cyprinus carpio*) to disturbance by Eurasian otter (*Lutra lutra*). *Fish Physiology and Biochemistry*, 34, 223–234.

R Core Team (2016). R: A language and environment for statistical computing. R Foundation for Statistical Computing, Vienna, Austria. URL https://www.R-project.org/.

Rau, A., Gallopin, M., Celeux, G. and Jaffrezic, F. (2013). Data-based filtering for replicated high-throughput transcriptome sequencing experiments. *Bioinformatics*, 29(17), 2146–2152.

Ray, R. and Miller, D. M. (1991). Cloning and characterization of a human c-*myc* promoter-binding protein. *Molecular and Cellular Biology*, 11(4), 2154–2161.

Reiling, J. H. and Sabatini, D. M. (2006). Stress and mTORture signaling. *Oncogene*, 25, 6373–6383.

Rey, S., Boltana, S., Vargas, R., Roher, N. and Mackenzie, S. (2013). Combining animal personalities with transcriptomics resolves individual variation within a wild-type zebrafish population and identifies underpinning molecular differences in brain function. *Molecular Ecology*, 22, 6100–6115.

Ricke, R. M. and Bielinsky, A-K. (2005). *Biological Procedures Online*, 7(1), 60–69.

Ritchie, M. E., Phipson, B., Wu, D., Hu, Y., Law, C. W., Shi, W., and Smyth, G. K. (2015). limma powers differential expression analyses for RNA-sequencing and microarray studies. *Nucleic Acids Research*, 43(7), e47.

Robinson, M. D., McCarthy, D. J. and Smyth, G. K. (2010). edgeR: a Bioconductor package for differential expression analysis of digital gene expression data. *Bioinformatics*, 26, 139–140.

Robinson, M. D. and Oshlack, A. (2010). A scaling normalization method for differential expression analysis of RNA-seq data. *Genome Biology*, 11, R25.

Rockstein, M. (1978). *Biochemistry of Insects*. New York, NY: Academic Press, INC.

Roeder, K. D. (1998). Nerve cells and insect behavior (revised edition). Harvard University Press, Cambridge, Massachusetts.

Roeder, K. D. (1966). Interneurons of the thoracic nerve cord activated by tympanic nerve fibres in noctuid moths. *Journal of Insect Physiology*, 12(10), 1227–1234.

Roeder, K. D. (1965). Moths and ultrasound. *Scientific American*, 212, 94–102.

Romer, H. and Bailey, W. (1996). Ecological constraints for the evolution of hearing and sound communication in insects. In *Evolutionary Biology of Hearing*, (ed. D. B. Webster, R. R. Fay and A. N. Popper), pp. 79–93. New York, NY: Springer.

Ross, T. S., Jefferson, A. B., Mitchell, C. A. and Majerus, P. W. Cloning and expression of human 75-kDa inositol polyphosphate-5-phosphatase. *Journal of Biological Chemistry*, 266(30), 20283–20289.

Roulin, A. C., Wu, M., Pichon, S., Arbore, R., Kuhn-Buhlmann, S., Kolliker, M. and Walser, J-C. (2014). *De novo* transcriptome hybrid assembly and validation in the european earwig

(Dermaptera, *Forficula auricularia*). *PLoS ONE*, 9(4), e94098. doi:10.1371/journal.pone.0094098.

Rovero, F., Hughes, R. N. and Chelazzi, G. (2000). When time is of the essence: choosing a currency for prey-handling costs. *Journal of Animal Ecology*, 69, 683–689.

Rowland, E., Belton, P., Schaefer, P. W. and Gries, G. (2014). Intraspecific acoustic communication and mechanical sensitivity of the tympanal ear of the gypsy moth *Lymantria dispar*. *Physiological Entomology*, 39(4), 331–340.

Rozenberg, A., Parida, M., Leese, F., Weiss, L. C., Tollrian, R. and Manak, J. R. (2015). Transcriptional profiling of predator-induced phenotypic plasticity in *Daphnia pulex*. *Frontiers in Zoology*, 12, 18.

Salinas, P. C. (2003). Synaptogenesis: Wnt and TGF- β take centre stage. *Current Biology*, 13(2), R60–R62.

Salisbury, J. P., Sirbulescu, R. F., Moran, B. M., Auclari, J. R., Zupanc, G. K. H. and Agar, J. N. (2015). The central nervous system transcriptome of the weakly electric brown ghost knifefish (*Apteronotus leptorhynchus*): *de novo* assembly, annotation and proteomics validation. *BMC Genomics*, 16, 166.

Samaraweera, P. and Law, J. H. (1995). Isolation, cloning and deduced amino acid sequence of a novel glycoprotein from the haemolymph of the hawkmoth *Manduca sexta*. *Insect Molecular Biology*, 4(1), 7–13.

Sanogo, Y. O., Hankison, S., Band, M., Obregon, A. and Bell, A. M. (2011). Brain transcriptomic response of threespine sticklebacks to cues of a predator. *Brains, Behavior, and Evolution*, 77, 270–285.

Schwarzenberger, A., Courts, C. and von Elert, E. (2009). Target gene approaches: Gene

expression in *Daphnia magna* exposed to predator-borne kairomones or to microcystin-producing and microcystin-free *Microcystis aeruginosa*. *BMC Genomics*, 10, 527.

Shah, M. A., Khan, A. A. and Mir, G. M. (2014). RNA interference for insect pest management-recent developments: a review. *Journal of Cell and Tissue Research*, 14(3), 4601–4608.

Shannon, P., Markiel, A., Ozier, O., Baliga, N. S., Wang, J. T., Ramage, D., Amin, N., Schwikowski, B. and Ideker, T. (2003). Cytoscape: a software environment for integrated models of biomolecular interaction networks. *Genome Research*, 13, 2498–2504.

Sims, S. R. (1998). A freeze-thaw stable diet for Lepidoptera. *Journal of Agricultural Entomology*, 15(1), 39–42.

Sinakevitch, I., Farris, S. M. and Strausfeld, N. J. (2001). Taurine-, aspartate- and glutamate-like immunoreactivity identifies chemically distinct subdivisions of Kenyon cells in the cockroach mushroom body. *Journal of Comparative Neurology*, 439, 352–367.

Slos, S. and Stoks, R. (2008). Predation risk induces stress proteins and reduces antioxidant defense. *Functional Ecology*, 22, 637–642.

Smith-Unna, R., Boursnell, C., Patro, R., Hibberd, J. M. and Kelly, S. (2015). *TransRate*: reference free quality assessment of *de-novo* transcriptome assemblies. *bioRxiv.org*, doi: http://dx.doi.org/10.1101/021626.

Smyth, G. K. (2004). Linear models and empirical Bayes methods for assessing differential expression in microarray experiments. *Statistical Applications in Genetics and Molecular Biology*, 3(1), 3.

Sourer, M. A., Khamiss, O., Abd El-Wahab, A. S., El-Sheikh, A. K. and Abul-Ela, S. (2011). An economically modified semi-synthetic diet for mass rearing the Egyptian cotton leaf worm *Spodoptera littoralis*. *Academic Journal of Entomology*, 4(3), 118–123.

Spangler, H. G. (1988). Hearing in tiger beetles (Cicindelidae). *Physiological Entomology*, 13, 447–452.

Spanier, K. I., Leese, F., Mayer, C., Colbourne, J. K., Gilbert, D., Pfender, M. E. and Tollrian, R. (2010). Predator-induced defenses in *Daphnia pulex*: Selection and evaluation of internal reference genes for gene expression studies with real-time PCR. *BMC Molecular Biology*, 11, 50.

Stelinski, L., Holdcraft, R. and Rodriguez-Saona, C. (2014). Female moth calling and flight behavior are altered hours following pheromone autodetection: possible implications for practical management with mating disruption. *Insects*, 5, 459–473.

Storey, J. D. (2004). Strong control, conservative point estimation and simultaneous conservative consistency of false discovery rates: a unified approach. *Journal of the Royal Statistical Society* B, 66(1), 187–205.

Surlykke, A. (1984). Hearing in notodontid moths: A tympanic organ with a single auditory neurone. *Journal of Experimental Biology*, 113: 323–335.

Surlykke, A. and Kalko, E. K. V. (2008). Echolocating bats cry out loud to detect their prey. *PLoS ONE*, 3(4), e2036. doi: 0.1371/journal.pone.0002036.

Surlykke, A. and Miller, L. A. (1982). Central branchings of three sensory axons from a moth ear (*Agrotis segetum*, Noctuidae). *Journal of Insect Physiology*, 28(4), 357–364.

Thaker, M., Lima, S. L., and Hews, D. K. (2009). Alternative antipredator tactics in tree lizard morphs: hormonal and behavioural responses to a predator encounter. *Animal Behaviour*, 77, 395–401.

Torkkeli, P. H., Liu, H. and French, A. S. (2015). Transcriptome analysis of the central and peripheral nervous systems of the spider *Cupiennius salei* reveals multiple putative cys-loop ligand gated ion channel subunits and acetylcholine binding protein. *PLoS ONE*, 10(9), e0138068. doi:10.1371/journal.pone.0138068.

Ulrich, J., Dao, V. A., Majumdar, U., Schmitt-Engel, C., Schwirz, J., Schultheis, D., Strohlen, N., Troelenberg, N., Grossmann, D., Richter, T., Donitz, J., Gerischer, L., Leboulle, G., Vilcinskas, A., Stanke, M. and Bucher, G. (2015). Large scale RNAi screen in *Tribolium* reveals novel target genes for pest control and the proteasome as prime target. *BMC Genomics*, 16, 674.

UniProt Consortium. (2013). Update on activities at the Universal Protein Resource (UniProt) in 2013. *Nucleic Acid Research*, 41, D43–D47.

Van Buskirk, J., Krugel, A., Kunz, J., Miss, F. and Stamm, A. (2014). The rate of degradation of chemical cues indicating predation risk: an experiment and review. *Ethology*, 120(9), 942–949.

Vanyushin, B. F., Belozersky, A. N., Kokurina, N. A. and Kadirova, D. X. (1968). 5-methylcytosine and 6-methylamino-purine in bacterial DNA. *Nature*, 218, 1066–1067.

Wang, C., Cao, Y. Wang, Z., Peng, G., Li, Z., Zhao, H. and Xia, Y. (2007). Differentially-expressed glycoproteins in *Locusta migratoria* hemolymph infected with *Metarhizium anisopliae*. *Journal of Invertebrate Pathology*, 96(3), 230–236.

Waters, D. A. & G. Jones. 1996. The peripheral auditory characteristics of noctuid moths: responses to the search-phase echolocation calls of bats. *Journal of Experimental Biology*, 199, 847–856.

Watkins, P. A., Maiguel, D., Jia, Z. and Pevsner, J. (2007). Evidence for 26 distinct acyl-coenzyme A synthetase genes in the human genome. *Journal of Lipid Research*, 48(12), 2736–2750.

Wnuk, A., Kostowski, W., Korczynska, J., Szczuka, A., Symonowicz, B., Bienkowski, P., Mierzejewski, P. and Godzinska, E. J. (2014). Brain GABA and glutamate levels in workers of two ant species (Hymenoptera: Formicidae): Interspecific differences and effects of queen presence/absence. *Insect Science*, 21, 647–658.

Yager, D. D., May, M. L. and Fenton, M. B. (1990). Ultrasound-triggered, flight-gated evasive maneuvers in the praying mantis *Parasphendale agrionina* I. Free flight. *Journal of Experimental Biology*, 152, 17–39.

Yager, D. D. and Svenson, G. J. (2008). Patterns of praying mantis auditory evolution based on morphological, molecular, neurophysiological, and behavioural data. *Biological Journal of the Linnean Society*, 94(3), 541–568.

Yamada, S., Pokutta, S., Drees, F., Weis, W. and Nelson, W. J. (2005). Deconstructing the cadherin-catenin-actin complex. *Cell*, 123(5), 889–901.

Yoshikawa, S., McKinnon, R. D., Kokei, M. and Thomas, J. B. (2003). Wnt-mediated axon guidance via the *Drosophila* Derailed receptor. *Nature*, 422, 583–588.

Zha, Y-P., Xu, F., Chen, Q-C., and Lei, C-L. (2008). Effect of ultrasound on acetylcholinesterase activity in *Helicoverpa armigera* (Lepidoptera: Noctuidae). *The Canadian Entomologist* 140, 563–568.

Zha, Y. P. and Lei, C. L. (2012). Effects of ultrasound-stress on antioxidant enzyme activities of *Helicoverpa armigera* (Hubner) (Lepidoptera: Noctuidae). *Journal of Agricultural and Urban Entomology*, 28, 34–41.

Zha, Y-P., Chen, J-Y., Jin, Z-B., Wang, C-B. and Lei, C-L. (2013). Effects of ultrasound on the fecundity and development of the cotton bollworm, *Helicoverpa Armigera* (Hübner) (Lepidoptera: Noctuidae). *Journal of Agricultural and Urban Entomology*, 29(1), 93–98.

Zhang, G., Huang, H., Liu, D., Cheng, Y., Liu, X., Zhang, W., Yin, R., Zhang, D., Zhang, P., Liu, J., Li, C., Liu, B., Luo, Y., Zhu, Y., Zhang, N., He, S., He, C., Wang, H. and Chen, D. (2015). N^6-methyladenine DNA modification in *Drosophila*. *Cell*, 161(4), 893–906.

Zhang, H., Li, H-C. and Miao, X-X. (2013). Feasability, limitation and possible solutions of RNAi-based technology for insect pest control. *Insect Science*, 20, 15–30.

Zou, Y. (2004). Wnt signaling in axon guidance. *Trends in Neuroscience*, 27(9), 528–532.

TABLES AND FIGURES

Table 1. Total RNA concentration, absorbance values, absorbance ratios, and RNA Integrity Number (RIN) for each brain tissue RNA extraction from control (C) and bat-ultrasound exposed (E) adult male *Spodoptera frugiperda* moths.

Sample ID	NanoDrop concentration (ng/uL)	Qubit concentration (ng/uL)	A260	A280	A260/280	RIN
C1	49.65	49.7	1.241	0.593	2.09	8.3
C2	54.78	58.4	1.37	0.636	2.15	8.5
C3	42.76	44.2	1.069	0.491	2.18	8.7
C4	46.21	49.1	1.155	0.539	2.14	8.3
E1	74.34	71.8	1.859	0.869	2.14	8.7
E2	52.91	56.6	1.323	0.638	2.07	8.8
E3	66.32	61.9	1.658	0.768	2.16	8.7
E4	35.29	38.1	0.882	0.419	2.11	9

Table 2. List of differentially upregulated transcripts recovered from brain tissue RNA extractions in bat-ultrasound exposed *Spodoptera frugiperda* adult male moths relative to control moths; relative expression estimates reported as fold-change (log_2), the most significant (e-value < 1e-5) BLASTX protein annotation statistics based on the UniRef90 database (UniProt Consortium, 2013), and the organism from which the annotation derived are included.

Transcript ID	Log_2 Fold Change	Ave. Expression	P Value	FDR-Adjusted P Value	Top UniRef90 BLASTX Hit	E-value	Organism
TRINITY_DN2230_c0_g1_i1	11.4500	-1.4769	0.0000	0.0000	-	-	-
TRINITY_DN37212_c0_g1_i3	9.8601	-0.7439	0.0000	0.0000	X-linked retinitis pigmentosa GTPase regulator homolog	0	*Bombyx mori*
TRINITY_DN36403_c0_g1_i3	9.6654	-2.1606	0.0000	0.0000	calcium uniporter protein mitochondrial	0	*Papilio polytes*
TRINITY_DN30280_c6_g1_i3	9.6383	-1.3637	0.0000	0.0000	-	-	-
TRINITY_DN38404_c0_g2_i3	9.5504	-1.0808	0.0000	0.0000	-	-	-
TRINITY_DN33318_c7_g1_i1	9.4738	-2.2233	0.0000	0.0000	-	-	-
TRINITY_DN33671_c2_g1_i8	9.3876	-1.2532	0.0000	0.0000	-	-	-
TRINITY_DN35646_c2_g4_i3	9.0219	-1.4826	0.0003	0.0594	uncharacterized protein LOC105386011	1.00E-43	*Plutella xylostella*
TRINITY_DN37234_c0_g1_i10	8.6926	-2.5344	0.0000	0.0000	-	-	-
TRINITY_DN30400_c2_g1_i4	8.6099	-2.5413	0.0000	0.0000	-	-	-
TRINITY_DN38739_c1_g1_i16	8.5436	-1.2902	0.0000	0.0000	protein polybromo-1	0	*Papilio* sp.
TRINITY_DN35646_c2_g4_i5	8.4296	-2.0614	0.0000	0.0130	uncharacterized protein LOC105386011	4.00E-42	*Plutella xylostella*
TRINITY_DN34405_c8_g8_i2	8.4089	-2.3193	0.0000	0.0000	-	-	-
TRINITY_DN40154_c8_g1_i2	8.2644	-1.0302	0.0000	0.0030	-	-	-
TRINITY_DN37042_c2_g2_i1	8.1724	-2.2874	0.0000	0.0006	-	-	-
TRINITY_DN40225_c4_g3_i1	7.9335	-2.4214	0.0000	0.0000	-	-	-
TRINITY_DN37134_c1_g1_i13	7.7773	-0.8312	0.0000	0.0111	-	-	-
TRINITY_DN34896_c2_g1_i1	7.7609	-2.3763	0.0000	0.0017	-	-	-
TRINITY_DN37497_c1_g1_i16	7.7348	-2.7427	0.0000	0.0024	nuclear factor 1 C-type-like	0	*Plutella xylostella*
TRINITY_DN33065_c0_g2_i1	7.7268	-2.6286	0.0000	0.0008	aminoacylase-1-like	1.00E-92	*Amyelois transitella*
TRINITY_DN32642_c3_g3_i12	7.6793	-2.1043	0.0000	0.0000	Regulatory-associated protein of TOR	0	*Bombyx mori*

Table 2 continued.

Transcript ID	Log_2 Fold Change	Ave. Expression	P Value	FDR-Adjusted P Value	Top UniRef90 BLASTX Hit	E-value	Organism
TRINITY_DN38729_c4_g1_i3	7.3105	-0.6533	0.0002	0.0484	phosphatidate cytidylyltransferase	0	*Ditrysia* sp.
TRINITY_DN36166_c2_g1_i1	7.1246	-2.2272	0.0000	0.0000	-	-	-
TRINITY_DN29778_c0_g1_i3	7.1124	-2.3090	0.0000	0.0077	-	-	-
TRINITY_DN31620_c0_g1_i6	7.0401	-3.2045	0.0000	0.0007	uncharacterized protein	0	*Papilio* sp.
TRINITY_DN34936_c0_g1_i3	6.9579	-2.4491	0.0000	0.0010	myoneurin-like	1.00E-76	*Bombyx mori*
TRINITY_DN37234_c0_g1_i8	6.8524	-2.5641	0.0000	0.0012	-	-	-
TRINITY_DN29467_c1_g1_i4	6.8383	-2.4531	0.0000	0.0000	-	-	-
TRINITY_DN25058_c0_g1_i3	6.8317	-3.0539	0.0000	0.0000	putative ecdysone oxidase	2.00E-15	*Operophtera brumata*
TRINITY_DN25058_c0_g1_i2	6.7810	-3.2099	0.0000	0.0000	mitochondrial choline dehydrogenase	3.00E-21	*Operophtera brumata*
TRINITY_DN36104_c1_g1_i1	6.7539	-1.9239	0.0000	0.0037	pro-resilin-like	2.00E-17	*Amyelois transitella*
TRINITY_DN37496_c0_g1_i3	6.7062	-2.3284	0.0000	0.0000	-	-	-
TRINITY_DN36563_c0_g1_i5	6.6760	-2.0072	0.0000	0.0149	Axin	0	*Papilio* sp.
TRINITY_DN37270_c2_g1_i4	6.6685	-2.6072	0.0001	0.0178	-	-	-
TRINITY_DN39071_c0_g1_i2	6.6680	-3.4169	0.0000	0.0088	putative uncharacterized protein	0	*Tribolium castaneum*
TRINITY_DN39461_c2_g2_i3	6.5369	-3.3048	0.0000	0.0000	-	-	-
TRINITY_DN39385_c2_g1_i1	6.4561	0.4404	0.0000	0.0007	-	-	-
TRINITY_DN36280_c3_g1_i10	6.4352	-1.6074	0.0001	0.0339	putative uncharacterized protein	3.00E-08	*Culex quinquefasciatus*
TRINITY_DN37496_c0_g1_i4	6.4322	-2.7123	0.0000	0.0000	-	-	-
TRINITY_DN37496_c0_g1_i6	6.3548	-2.6646	0.0000	0.0000	-	-	-
TRINITY_DN37496_c0_g2_i12	6.3394	-2.4473	0.0000	0.0000	uncharacterized protein	2.00E-96	*Danaus plexippus*
TRINITY_DN37877_c0_g1_i2	6.3218	-3.3586	0.0000	0.0004	-	-	-
TRINITY_DN30964_c1_g2_i5	6.3073	-2.7133	0.0000	0.0002	ester hydrolase C11orf54 homolog	3.00E-136	*Amyelois transitella*
TRINITY_DN34741_c4_g2_i4	6.2842	-3.2922	0.0001	0.0191	-	-	-
TRINITY_DN37496_c0_g1_i10	6.2575	-2.7025	0.0000	0.0000	-	-	-

Table 2 continued.

Transcript ID	Log_2 Fold Change	Ave. Expression	P Value	FDR-Adjusted P Value	Top UniRef90 BLASTX Hit	E-value	Organism
TRINITY_DN40271_c4_g1_i5	6.2438	-3.0788	0.0000	0.0004	-	-	-
TRINITY_DN38404_c0_g2_i2	6.2234	-2.7265	0.0000	0.0000	acyl-CoA synthetase short-chain family member 3 mitochondrial	0	*Amyelois transitella*
TRINITY_DN32565_c0_g2_i3	6.2016	-2.6574	0.0000	0.0000	-	-	-
TRINITY_DN39907_c0_g1_i3	6.1037	-2.8112	0.0001	0.0207	coronin-6 isoform X1	0	*Obtectomera* sp.
TRINITY_DN37997_c0_g1_i2	6.0595	-2.4577	0.0000	0.0001	type II inositol 1 4 5-trisphosphate 5-phosphatase	0	*Papilio* sp.
TRINITY_DN31620_c0_g1_i1	6.0511	-3.5720	0.0000	0.0002	uncharacterized protein	0	*Papilio* sp.
TRINITY_DN37364_c0_g5_i1	5.9831	-3.5345	0.0000	0.0000	cystinosin homolog isoform X1	3.00E-12	*Plutella xylostella*
TRINITY_DN38655_c0_g1_i1	5.9808	-3.0258	0.0000	0.0078	ATP-binding cassette sub-family G member 5	0	*Bombyx mori*
TRINITY_DN32711_c0_g1_i3	5.9679	-2.9031	0.0000	0.0007	doublesex- and mab-3-related transcription factor 3	6.00E-134	*Amyelois transitella*
TRINITY_DN29332_c0_g1_i3	5.8838	-3.1589	0.0000	0.0027	-	-	-
TRINITY_DN35731_c2_g1_i1	5.8568	-1.1235	0.0002	0.0488	-	-	-
TRINITY_DN39575_c4_g3_i5	5.8164	-3.7350	0.0001	0.0360	-	-	-
TRINITY_DN33671_c2_g1_i7	5.7500	-3.1041	0.0000	0.0000	-	-	-
TRINITY_DN27959_c1_g1_i1	5.7076	-3.3723	0.0000	0.0004	uncharacterized protein	7.00E-98	*Bombyx mori*
TRINITY_DN30778_c0_g1_i4	5.6997	-2.5512	0.0001	0.0233	putative chemosensory ionotropic receptor IR75d (Fragment)	0	*Spodoptera littoralis*
TRINITY_DN33595_c2_g1_i8	5.6920	-2.9806	0.0000	0.0001	uncharacterized protein	0	*Bombyx mori*
TRINITY_DN37234_c0_g2_i1	5.6403	-2.9497	0.0000	0.0023	-	-	-
TRINITY_DN37848_c1_g3_i6	5.6040	-3.0244	0.0000	0.0000	mutant cadherin	8.00E-16	*Helicoverpa armigera*
TRINITY_DN16945_c0_g1_i1	5.4814	-3.4197	0.0000	0.0016	-	-	-
TRINITY_DN37364_c0_g1_i1	5.4556	-3.7441	0.0000	0.0000	-	-	-
TRINITY_DN38899_c0_g1_i1	5.2744	4.5685	0.0000	0.0016	uncharacterized protein	8.00E-168	*Danaus plexippus*
TRINITY_DN38884_c1_g1_i5	5.1372	-3.8241	0.0000	0.0009	-	-	-

Table 2 continued.

Transcript ID	Log_2 Fold Change	Ave. Expression	P Value	FDR-Adjusted P Value	Top UniRef90 BLASTX Hit	E-value	Organism
TRINITY_DN33012_c0_g1_i2	5.1079	-1.6502	0.0000	0.0134	-	-	-
TRINITY_DN37390_c4_g4_i3	5.0402	-3.2212	0.0001	0.0341	-	-	-
TRINITY_DN33831_c3_g1_i12	5.0258	-3.2425	0.0001	0.0177	-	-	-
TRINITY_DN38345_c0_g1_i5	4.9378	-3.2726	0.0000	0.0016	dorsal 1a	5.00E-100	*Spodoptera litura*
TRINITY_DN40225_c4_g3_i3	4.8838	-2.1985	0.0000	0.0100	-	-	-
TRINITY_DN36290_c2_g1_i3	4.8566	-3.2157	0.0000	0.0003	-	-	-
TRINITY_DN39385_c0_g1_i1	4.8501	1.4926	0.0000	0.0001	-	-	-
TRINITY_DN32186_c0_g1_i3	4.7616	-1.9394	0.0001	0.0286	-	-	-
TRINITY_DN37042_c3_g1_i2	4.6684	-2.2283	0.0000	0.0032	-	-	-
TRINITY_DN35392_c2_g1_i10	4.6570	-3.2271	0.0001	0.0308	uncharacterized protein LOC107191251	8.00E-94	*Dufourea novaeangliae*
TRINITY_DN33705_c1_g1_i5	4.6475	-3.9626	0.0002	0.0392	synaptic vesicle glycoprotein 2B-like	1.00E-112	*Amyelois transitella*
TRINITY_DN38135_c7_g3_i1	4.6201	-2.5497	0.0001	0.0266	-	-	-
TRINITY_DN33081_c0_g1_i4	4.6060	-2.4724	0.0001	0.0320	dual specificity protein phosphatase 18	4.00E-28	*Operophtera brumata*
TRINITY_DN36290_c2_g1_i9	4.4223	-2.1098	0.0000	0.0061	sodium/potassium-transporting ATPase subunit beta-2-like	6.00E-19	*Amyelois transitella*
TRINITY_DN38768_c0_g1_i1	4.3666	-0.2316	0.0000	0.0035	uncharacterized protein LOC106125418	7.00E-147	*Papilio* sp.
TRINITY_DN40225_c4_g3_i4	4.3080	1.0204	0.0000	0.0024	-	-	-
TRINITY_DN35309_c0_g1_i1	4.2933	-1.4013	0.0003	0.0654	uncharacterized protein LOC105383334	2.00E-52	*Plutella xylostella*
TRINITY_DN39696_c4_g6_i1	4.2733	-3.4922	0.0001	0.0201	-	-	-
TRINITY_DN39395_c1_g1_i5	4.1823	-3.4153	0.0000	0.0002	serine/arginine repetitive matrix protein 1-like isoform X1	6.00E-135	*Papilio xuthus*
TRINITY_DN39527_c0_g1_i11	3.7373	6.2709	0.0000	0.0027	Z band alternatively spliced PDZ-motif protein 66	1.00E-41	*Papilio xuthus*
TRINITY_DN38817_c2_g2_i4	3.6350	-2.4653	0.0001	0.0233	uncharacterized protein (Fragment)	1.00E-94	*Pararge aegeria*
TRINITY_DN38768_c0_g1_i3	3.4858	1.2063	0.0000	0.0023	uncharacterized protein LOC106125418	3.00E-86	*Papilio* sp.
TRINITY_DN37183_c3_g1_i4	3.4076	3.6403	0.0001	0.0269	-	-	-

Table 2 continued.

Transcript ID	Log_2 Fold Change	Ave. Expression	P Value	FDR-Adjusted P Value	Top UniRef90 BLASTX Hit	E-value	Organism
TRINITY_DN31771_c5_g1_i1	3.3905	-3.4420	0.0002	0.0363	-	-	-
TRINITY_DN36952_c0_g1_i7	3.3250	-1.6521	0.0001	0.0191	cytochrome CYP341B3	0	*Spodoptera littoralis*
TRINITY_DN25843_c0_g2_i1	2.9305	-0.9304	0.0000	0.0134	-	-	-
TRINITY_DN39385_c1_g2_i2	2.8797	-1.0180	0.0001	0.0214	-	-	-
TRINITY_DN39461_c2_g2_i6	2.8066	0.9131	0.0000	0.0093	-	-	-
TRINITY_DN31963_c0_g1_i4	2.7588	-2.9390	0.0001	0.0238	-	-	-
TRINITY_DN36997_c1_g1_i5	2.6367	2.6586	0.0002	0.0402	-	-	-
TRINITY_DN39518_c1_g1_i3	2.6160	1.7318	0.0002	0.0431	ATP-binding cassette sub-family G member 8	0	*Amyelois transitella*
TRINITY_DN37039_c2_g2_i5	2.5625	0.4671	0.0002	0.0484	phosphatidylglycerophosphatase and protein-tyrosine phosphatase 1	5.00E-123	*Amyelois transitella*
TRINITY_DN35489_c0_g1_i7	2.4620	2.2836	0.0000	0.0052	-	-	-
TRINITY_DN39905_c2_g3_i1	2.3712	-0.0139	0.0000	0.0077	-	-	-
TRINITY_DN35975_c0_g1_i7	2.3211	-0.8273	0.0000	0.0025	protein Gawky	0	*Papilio* sp.
TRINITY_DN35944_c2_g2_i1	2.3075	-3.1464	0.0001	0.0290	uncharacterized protein	3.00E-10	*Papilio xuthus*
TRINITY_DN40277_c8_g2_i4	2.0996	-0.4446	0.0001	0.0237	uncharacterized protein LOC106713896 partial	2.00E-19	*Papilio machaon*
TRINITY_DN33887_c0_g2_i12	1.9515	-1.5605	0.0001	0.0237	ubiquitin (fragment)	2.00E-57	*Protostomia* sp.
TRINITY_DN37783_c3_g1_i2	1.8835	-3.4846	0.0000	0.0061	-	-	-
TRINITY_DN30635_c2_g1_i1	1.8800	0.3746	0.0002	0.0495	REPAT30	2.00E-63	*Spodoptera* sp.
TRINITY_DN32840_c2_g1_i2	1.8271	-0.6562	0.0001	0.0248	-	-	-
TRINITY_DN39967_c1_g1_i5	1.7884	2.2680	0.0001	0.0314	cytoplasmic dynein 1 intermediate chain isoform X8	0	*Amyelois transitella*
TRINITY_DN39493_c0_g3_i1	1.7112	-0.6333	0.0002	0.0393	rho GTPase-activating protein 190-like	6.00E-44	*Plutella xylostella*
TRINITY_DN38296_c0_g1_i4	1.5741	0.0926	0.0001	0.0207	uncharacterized protein	1.00E-103	*Danaus plexippus*
TRINITY_DN37877_c0_g1_i22	1.5721	-4.2336	0.2917	0.6661	-	-	-

Table 2 continued.

Transcript ID	Log_2 Fold Change	Ave. Expression	P Value	FDR-Adjusted P Value	Top UniRef90 BLASTX Hit	E-value	Organism
TRINITY_DN39931_c0_g1_i9	1.5383	1.9613	0.0002	0.0415	uncharacterized protein LOC101741686	0	*Bombyx mori*
TRINITY_DN37435_c0_g1_i4	1.3806	4.7764	0.0001	0.0298	casein kinase I isoform gamma-3	0	*Pongo abelii*
TRINITY_DN33003_c3_g1_i2	1.2936	5.2805	0.0002	0.0438	-	-	-

Table 3. List of down-regulated transcripts recovered from brain tissue RNA extractions in bat-ultrasound exposed *Spodoptera frugiperda* adult male moths relative to control moths; relative expression estimates reported as fold-change (log_2), the most significant (e-value < 1e-5) BLASTX protein annotation statistics based on the UniRef90 database (UniProt Consortium, 2013), and the organism from which the annotation derived are included.

Transcript ID	Log_2 Fold Change	Ave. Expression	P Value	FDR-Adjusted P Value	Top UniRef90 BLASTX Hit	E-value	Organism
TRINITY_DN22838_c0_g2_i1	-10.5503	0.8597	0.0000	0.0000	-	-	-
TRINITY_DN34268_c3_g1_i3	-10.3989	-0.6024	0.0000	0.0000	27 kDa hemolymph protein	5.00E-90	*Pararge aegeria*
TRINITY_DN40225_c4_g3_i5	-10.3616	-0.3944	0.0000	0.0001	-	-	-
TRINITY_DN34268_c4_g1_i1	-10.1455	-0.6638	0.0000	0.0000	-	-	-
TRINITY_DN25356_c0_g2_i1	-9.7357	0.4281	0.0000	0.0000	-	-	-
TRINITY_DN38145_c1_g1_i1	-9.4768	0.0648	0.0000	0.0000	-	-	-
TRINITY_DN38793_c0_g2_i2	-9.3882	-0.2339	0.0002	0.0498	equilibrative nucleoside transporter	0	*Pararge aegeria*
TRINITY_DN36116_c4_g2_i6	-9.3085	-0.4714	0.0000	0.0008	-	-	-
TRINITY_DN38739_c1_g1_i5	-9.1023	-1.2984	0.0000	0.0000	protein polybromo-1	0	*Papilio* sp.
TRINITY_DN33671_c2_g1_i1	-9.0696	-1.3407	0.0000	0.0000	-	-	-
TRINITY_DN32305_c5_g1_i3	-8.8475	-0.6495	0.0000	0.0042	-	-	-
TRINITY_DN35489_c0_g1_i6	-8.8298	-1.4900	0.0000	0.0003	-	-	-
TRINITY_DN24438_c0_g2_i1	-8.7905	1.2303	0.0000	0.0003	-	-	-
TRINITY_DN33318_c7_g1_i4	-8.7839	-1.2434	0.0000	0.0001	-	-	-
TRINITY_DN37153_c0_g3_i7	-8.6013	-1.5878	0.0000	0.0001	LOW QUALITY PROTEIN voltage-dependent T-type calcium channel subunit alpha-1G	0	*Bombyx mori*
TRINITY_DN29335_c0_g1_i1	-8.5909	-1.4573	0.0000	0.0000	uncharacterized protein LOC106129727	4.00E-36	*Amyelois transitella*
TRINITY_DN33003_c2_g1_i2	-8.5809	-0.4078	0.0000	0.0000	-	-	-
TRINITY_DN38739_c1_g1_i1	-8.5236	-1.5621	0.0000	0.0001	protein polybromo-1	0	*Papilio* sp.
TRINITY_DN37612_c0_g1_i1	-8.4772	-1.6945	0.0001	0.0233	peripheral-type benzodiazepine receptor isoform X1	4.00E-83	*Bombyx mori*

Table 3 continued.

Transcript ID	Log_2 Fold Change	Ave. Expression	P Value	FDR-Adjusted P Value	Top UniRef90 BLASTX Hit	E-value	Organism
TRINITY_DN32142_c0_g2_i1	-8.4481	-1.5247	0.0000	0.0000	-	-	-
TRINITY_DN36507_c0_g1_i5	-8.4379	-0.1039	0.0001	0.0313	-	-	-
TRINITY_DN38898_c0_g1_i4	-8.3471	-0.2149	0.0000	0.0001	ADP ribosylation factor	1.00E-107	*Oryctes borbonicus*
TRINITY_DN37203_c0_g1_i2	-8.3042	-1.6302	0.0000	0.0000	integrin beta pat-3	1.00E-100	*Danaus plexippus*
TRINITY_DN30280_c6_g1_i2	-8.1934	1.1569	0.0000	0.0047	-	-	-
TRINITY_DN35996_c6_g2_i7	-8.1751	-0.4905	0.0000	0.0002	uncharacterized protein	2.00E-120	*Operophtera brumata*
TRINITY_DN33703_c0_g1_i10	-7.8473	-0.8351	0.0000	0.0000	FH1/FH2 domain-containing protein 3	0	*Bombyx mori*
TRINITY_DN32368_c2_g1_i1	-7.8392	-1.7751	0.0000	0.0000	-	-	-
TRINITY_DN33037_c7_g1_i1	-7.7746	-0.7471	0.0000	0.0013	-	-	-
TRINITY_DN32675_c1_g1_i2	-7.7181	-0.5445	0.0000	0.0061	-	-	-
TRINITY_DN35308_c0_g7_i2	-7.6312	-1.8407	0.0000	0.0000	uncharacterized protein LOC106143546	0	*Amyelois transitella*
TRINITY_DN32480_c1_g1_i2	-7.6141	-1.7956	0.0000	0.0003	-	-	-
TRINITY_DN38739_c1_g1_i4	-7.5996	-1.8992	0.0000	0.0003	protein polybromo-1	0	*Papilio* sp.
TRINITY_DN30400_c2_g1_i3	-7.5346	-1.9257	0.0000	0.0001	-	-	-
TRINITY_DN32071_c5_g2_i3	-7.5332	-0.9221	0.0000	0.0124	-	-	-
TRINITY_DN35282_c3_g2_i3	-7.5319	-1.5419	0.0001	0.0313	2-methylene-furan-3-one reductase-like	0	*Bombyx mori*
TRINITY_DN39284_c17_g3_i1	-7.5016	-1.1912	0.0000	0.0001	uncharacterized protein	4.00E-19	*Danaus plexippus*
TRINITY_DN36116_c4_g2_i3	-7.4942	-0.4979	0.0001	0.0332	-	-	-
TRINITY_DN37745_c1_g3_i1	-7.4529	-2.0874	0.0000	0.0000	-	-	-
TRINITY_DN38739_c1_g1_i12	-7.3904	-2.1667	0.0000	0.0014	protein polybromo-1	0	*Papilio* sp.
TRINITY_DN32480_c1_g1_i1	-7.3853	-2.0826	0.0000	0.0000	-	-	-
TRINITY_DN35996_c6_g3_i1	-7.3769	-1.0123	0.0000	0.0009	-	-	-
TRINITY_DN37270_c2_g1_i3	-7.3114	-2.1964	0.0000	0.0001	-	-	-
TRINITY_DN37446_c0_g1_i5	-7.2694	-0.5738	0.0002	0.0435	-	-	-

Table 3 continued.

Transcript ID	Log_2 Fold Change	Ave. Expression	P Value	FDR-Adjusted P Value	Top UniRef90 BLASTX Hit	E-value	Organism
TRINITY_DN34464_c1_g2_i7	-7.2006	-1.3360	0.0000	0.0008	Kv channel-interacting protein 4-like	2.00E-112	*Amyelois transitella*
TRINITY_DN34160_c1_g2_i1	-7.1791	-1.1829	0.0000	0.0000	DNA N6-methyl adenine demethylase-like isoform X1	2.00E-48	*Amyelois transitella*
TRINITY_DN35932_c1_g2_i2	-7.1349	-2.5094	0.0001	0.0308	uncharacterized protein LOC106133073 isoform X1	8.00E-133	*Amyelois transitella*
TRINITY_DN32911_c0_g2_i1	-7.0475	-1.7120	0.0000	0.0001	-	-	-
TRINITY_DN38739_c1_g1_i14	-6.9385	-1.9898	0.0000	0.0000	protein polybromo-1	0	*Papilio* sp.
TRINITY_DN39310_c1_g2_i4	-6.9376	-0.1062	0.0000	0.0024	ankyrin repeat domain-containing protein 17-like	1.00E-121	*Papilio xuthus*
TRINITY_DN36781_c3_g1_i6	-6.9246	-1.4879	0.0002	0.0448	cytochrome P450	0	*Spodoptera litura*
TRINITY_DN38815_c3_g4_i6	-6.8984	0.0770	0.0000	0.0000	-	-	-
TRINITY_DN32730_c0_g1_i3	-6.8032	-1.5119	0.0000	0.0000	decaprenyl-diphosphate synthase subunit 2	0	*Amyelois transitella*
TRINITY_DN37877_c0_g1_i17	-6.7731	-1.4192	0.0000	0.0057	-	-	-
TRINITY_DN38024_c0_g2_i11	-6.7309	-1.2620	0.0000	0.0000	-	-	-
TRINITY_DN34405_c8_g4_i1	-6.7285	-1.5021	0.0000	0.0043	-	-	-
TRINITY_DN38296_c0_g1_i8	-6.7146	-1.4859	0.0000	0.0002	uncharacterized protein	7.00E-104	*Danaus plexippus*
TRINITY_DN19414_c1_g1_i1	-6.6813	-1.5167	0.0000	0.0000	glutamate synthase	3.00E-50	*Bombyx mori*
TRINITY_DN38328_c0_g1_i4	-6.6761	-2.2826	0.0000	0.0012	uncharacterized protein	0	*Danaus plexippus*
TRINITY_DN38884_c1_g1_i14	-6.6106	-1.1688	0.0000	0.0022	-	-	-
TRINITY_DN35288_c0_g5_i3	-6.5728	-1.2283	0.0001	0.0234	-	-	-
TRINITY_DN37832_c2_g1_i1	-6.5413	-1.5530	0.0000	0.0000	-	-	-
TRINITY_DN38898_c0_g1_i3	-6.5141	-1.6907	0.0000	0.0008	-	-	-
TRINITY_DN37781_c1_g1_i6	-6.4907	-2.0293	0.0000	0.0010	maltase 2-like isoform X1	4.00E-85	*Amyelois transitella*
TRINITY_DN32376_c4_g1_i4	-6.4609	-1.2338	0.0000	0.0009	-	-	-
TRINITY_DN33252_c1_g1_i3	-6.4412	-2.4937	0.0000	0.0000	-	-	-
TRINITY_DN36153_c0_g1_i3	-6.4325	-0.4561	0.0001	0.0254	guanine nucleotide-binding protein-like 3 homolog	1.00E-92	*Papilio* sp.

Table 3 continued.

Transcript ID	Log_2 Fold Change	Ave. Expression	P Value	FDR-Adjusted P Value	Top UniRef90 BLASTX Hit	E-value	Organism
TRINITY_DN30786_c0_g1_i4	-6.4324	-1.8255	0.0000	0.0000	-	-	-
TRINITY_DN34405_c8_g1_i1	-6.3667	-2.5342	0.0000	0.0002	-	-	-
TRINITY_DN38604_c4_g5_i2	-6.3565	-2.5853	0.0000	0.0000	-	-	-
TRINITY_DN34116_c1_g2_i1	-6.3322	-2.1255	0.0001	0.0167	uncharacterized protein	2.00E-118	*Acyrthosiphon pisum*
TRINITY_DN19813_c0_g1_i1	-6.2812	-2.6099	0.0000	0.0000	-	-	-
TRINITY_DN19414_c0_g1_i1	-6.2801	-1.5813	0.0000	0.0000	glutamate synthase NADH amyloplastic	6.00E-39	*Amyelois transitella*
TRINITY_DN32420_c1_g1_i2	-6.2359	-1.7600	0.0000	0.0001	-	-	-
TRINITY_DN34560_c0_g1_i3	-6.2113	-1.4242	0.0000	0.0009	integrin beta	0	*Spodoptera frugiperda*
TRINITY_DN39620_c1_g1_i1	-6.1933	-2.6925	0.0000	0.0000	-	-	-
TRINITY_DN39051_c0_g2_i4	-6.1856	-1.5023	0.0000	0.0003	uncharacterized protein	0	*Bombyx mori*
TRINITY_DN38145_c3_g1_i7	-6.1258	4.6107	0.0000	0.0007	uncharacterized protein	4.00E-64	*Bombyx mori*
TRINITY_DN39075_c0_g1_i3	-6.1197	-2.0518	0.0000	0.0057	uncharacterized protein	1.00E-82	*Bombyx mori*
TRINITY_DN37832_c3_g1_i1	-6.0722	-1.6664	0.0000	0.0036	-	-	-
TRINITY_DN32193_c2_g1_i4	-6.0557	-1.2068	0.0001	0.0284	mitoferrin-1-like	9.00E-74	*Plutella xylostella*
TRINITY_DN32223_c5_g5_i2	-5.9885	-2.7475	0.0000	0.0000	-	-	-
TRINITY_DN39620_c1_g1_i3	-5.9855	-2.7377	0.0000	0.0000	-	-	-
TRINITY_DN13201_c0_g2_i1	-5.9681	-2.8018	0.0000	0.0000	uncharacterized protein (Fragment)	7.00E-06	*Piscirickettsia salmonis*
TRINITY_DN32859_c0_g1_i5	-5.9676	-2.3071	0.0000	0.0021	putative pigeon protein	8.00E-97	*Danaus plexippus*
TRINITY_DN38145_c2_g1_i1	-5.9460	1.8448	0.0000	0.0001	-	-	-
TRINITY_DN40054_c3_g2_i4	-5.9348	-2.0780	0.0000	0.0001	WD repeat-containing protein 7 isoform X4	0	*Papilio* sp.
TRINITY_DN32169_c0_g1_i1	-5.9273	-2.4522	0.0000	0.0007	muscle segmentation homeobox-like	2.00E-125	*Amyelois transitella*
TRINITY_DN28597_c2_g1_i2	-5.8573	-2.7815	0.0000	0.0001	-	-	-
TRINITY_DN38225_c0_g1_i1	-5.7856	6.9465	0.0001	0.0174	-	-	-

Table 3 continued.

Transcript ID	Log_2 Fold Change	Ave. Expression	P Value	FDR-Adjusted P Value	Top UniRef90 BLASTX Hit	E-value	Organism
TRINITY_DN36707_c1_g1_i9	-5.7281	2.6878	0.0000	0.0001	small conductance calcium-activated potassium channel protein	0	*Papilio polytes*
TRINITY_DN38163_c1_g2_i3	-5.7064	-0.9392	0.0000	0.0000	catenin alpha	0	*Papilio polytes*
TRINITY_DN32901_c1_g5_i6	-5.6814	-2.8263	0.0000	0.0001	-	-	-
TRINITY_DN36307_c4_g1_i1	-5.6794	-2.9278	0.0000	0.0000	-	-	-
TRINITY_DN33558_c0_g2_i2	-5.6784	-1.7908	0.0000	0.0045	-	-	-
TRINITY_DN30964_c1_g2_i11	-5.6598	-2.8307	0.0000	0.0013	ester hydrolase C11orf54 homolog	4.00E-136	*Amyelois transitella*
TRINITY_DN29565_c0_g1_i2	-5.6537	-2.9354	0.0000	0.0007	-	-	-
TRINITY_DN29467_c1_g1_i2	-5.5721	-0.9144	0.0001	0.0233	-	-	-
TRINITY_DN32901_c1_g5_i5	-5.5703	-2.7745	0.0000	0.0054	-	-	-
TRINITY_DN39896_c1_g2_i9	-5.5700	-2.0328	0.0000	0.0036	-	-	-
TRINITY_DN34685_c1_g1_i7	-5.4612	-3.0575	0.0000	0.0001	laminin subunit alpha-1-like	2.00E-20	*Papilio machaon*
TRINITY_DN39620_c0_g1_i1	-5.4020	-3.0114	0.0000	0.0013	-	-	-
TRINITY_DN36528_c1_g3_i2	-5.3538	-0.7063	0.0001	0.0281	-	-	-
TRINITY_DN35630_c2_g1_i1	-5.3404	-2.3969	0.0002	0.0364	retrovirus-related Pol polyprotein from type-2 retrotransposable element R2DM	0	*Ceratitis capitata*
TRINITY_DN39032_c0_g1_i9	-5.3317	-0.2183	0.0000	0.0016	bromodomain-containing protein DDB_G0270170-like isoform X2	4.00E-133	*Papilio machaon*
TRINITY_DN38390_c0_g1_i4	-5.3096	-0.0925	0.0001	0.0209	phosphatidylinositol 5-phosphate 4-kinase type-2 beta	0	*Ditrysia* sp.
TRINITY_DN37365_c2_g1_i1	-5.2580	-2.0441	0.0001	0.0248	uncharacterized protein (Fragment)	1.00E-10	*Lottia gigantea*
TRINITY_DN32376_c4_g1_i2	-5.2177	-0.9262	0.0003	0.0586	-	-	-
TRINITY_DN39073_c3_g2_i13	-5.1049	-0.1081	0.0000	0.0141	ATP-citrate synthase	0	*Amyelois transitella*
TRINITY_DN37823_c2_g1_i8	-5.1015	-2.4653	0.0000	0.0001	omega-amidase NIT2-A isoform X1	2.00E-145	*Amyelois transitella*
TRINITY_DN32098_c6_g2_i5	-5.0548	-1.6991	0.0001	0.0308	-	-	-
TRINITY_DN37877_c0_g1_i9	-4.9263	-1.0798	0.0003	0.0551	-	-	-

Table 3 continued.

Transcript ID	Log_2 Fold Change	Ave. Expression	P Value	FDR-Adjusted P Value	Top UniRef90 BLASTX Hit	E-value	Organism
TRINITY_DN37877_c0_g1_i3	-4.9010	-1.0945	0.0001	0.0264	-	-	-
TRINITY_DN28575_c0_g1_i3	-4.8579	-2.8302	0.0000	0.0150	solute carrier family 12 member 4 isoform X3	2.00E-22	*Papilio* sp.
TRINITY_DN28328_c0_g1_i3	-4.8107	-0.5775	0.0001	0.0237	-	-	-
TRINITY_DN29816_c0_g1_i2	-4.7990	4.0335	0.0000	0.0030	-	-	-
TRINITY_DN33031_c2_g2_i1	-4.7372	-2.7559	0.0000	0.0036	-	-	-
TRINITY_DN39545_c3_g1_i15	-4.6986	-2.8005	0.0001	0.0308	endonuclease-reverse transcriptase	5.00E-21	*Bombyx mori*
TRINITY_DN31477_c1_g1_i4	-4.5937	-2.5111	0.0000	0.0149	formin-like protein 15	2.00E-07	*Papilio machaon*
TRINITY_DN31395_c1_g1_i7	-4.5928	-3.1908	0.0003	0.0561	arrestin homolog	0	*Obtectomera* sp.
TRINITY_DN34685_c1_g2_i2	-4.5483	-2.1143	0.0001	0.0309	zinc finger MYM-type protein 1-like	6.00E-40	*Hydra vulgaris*
TRINITY_DN40097_c0_g1_i1	-4.4741	0.6703	0.0000	0.0009	c-myc promoter-binding protein	0	*Homo sapiens*
TRINITY_DN38137_c0_g1_i4	-4.4587	-1.6514	0.0001	0.0360	atrial natriuretic peptide-converting enzyme	0	*Bombyx mori*
TRINITY_DN36274_c0_g1_i2	-4.4428	-0.1042	0.0000	0.0001	peptidyl-prolyl cis-trans isomerase FKBP65-like	5.00E-132	*Amyelois transitella*
TRINITY_DN37566_c0_g1_i2	-4.3099	-1.7781	0.0002	0.0444	-	-	-
TRINITY_DN35090_c0_g1_i3	-4.2946	-0.3012	0.0000	0.0043	uncharacterized protein	3.00E-165	*Bombyx mori*
TRINITY_DN34211_c0_g1_i3	-4.2249	1.0640	0.0001	0.0178	nuclear distribution protein NUDC	2.00E-161	*Biston betularia*
TRINITY_DN15012_c0_g2_i1	-4.1508	-1.2234	0.0001	0.0339	C-Cbl-associated protein isoform A	3.00E-10	*Operophtera brumata*
TRINITY_DN37270_c2_g1_i1	-4.1292	-3.6822	0.0002	0.0477	-	-	-
TRINITY_DN28005_c0_g1_i2	-4.1255	0.4174	0.0000	0.0017	39S ribosomal protein L34 mitochondrial	2.00E-36	*Papilio machaon*
TRINITY_DN28021_c0_g1_i1	-4.0897	-1.1177	0.0001	0.0233	Uncharacterized protein	3.00E-47	*Helobdella robusta*
TRINITY_DN40141_c1_g2_i1	-4.0186	-2.8432	0.0000	0.0010	glutamate synthase (Fragment)	5.00E-38	*Pararge aegeria*
TRINITY_DN39099_c2_g1_i1	-3.9941	2.8840	0.0000	0.0061	-	-	-

Table 3 continued.

Transcript ID	Log_2 Fold Change	Ave. Expression	P Value	FDR-Adjusted P Value	Top UniRef90 BLASTX Hit	E-value	Organism
TRINITY_DN36043_c0_g5_i1	-3.8734	-1.9678	0.0000	0.0091	-	-	-
TRINITY_DN37203_c0_g1_i3	-3.8576	3.1474	0.0000	0.0025	integrin beta pat-3	8.00E-94	*Danaus plexippus*
TRINITY_DN37133_c4_g2_i5	-3.8209	-1.1337	0.0002	0.0402	-	-	-
TRINITY_DN31324_c0_g1_i3	-3.7809	-2.0764	0.0001	0.0207	ubiquitin carboxyl-terminal hydrolase 34-like	2.00E-116	*Papilio machaon*
TRINITY_DN37153_c0_g3_i6	-3.6908	4.6006	0.0001	0.0207	LOW QUALITY PROTEIN voltage-dependent T-type calcium channel subunit alpha-1G	0	*Bombyx mori*
TRINITY_DN39970_c7_g3_i1	-3.6002	-2.2744	0.0000	0.0036	-	-	-
TRINITY_DN36698_c2_g1_i3	-3.5166	-2.5650	0.0002	0.0369	uncharacterized protein LOC106113347	3.00E-40	*Obtectomera* sp.
TRINITY_DN38059_c0_g1_i1	-3.4333	2.4478	0.0000	0.0053	putative acetyltransferase ACT11	8.00E-102	*Spodoptera litura*
TRINITY_DN40211_c8_g13_i2	-3.3949	-2.6487	0.0000	0.0012	uncharacterized protein	1.00E-17	*Piscirickettsia salmonis*
TRINITY_DN31644_c0_g1_i4	-3.2356	-1.6085	0.0000	0.0117	-	-	-
TRINITY_DN34933_c1_g1_i6	-3.1838	-1.7262	0.0000	0.0028	collagen alpha-1(XXV) chain-like isoform X8	6.00E-69	*Bombyx mori*
TRINITY_DN39085_c0_g1_i6	-3.1011	4.5699	0.0000	0.0034	LOW QUALITY PROTEIN uncharacterized protein LOC101738244	3.00E-153	*Bombyx mori*
TRINITY_DN33252_c1_g1_i1	-3.0698	2.3138	0.0000	0.0045	-	-	-
TRINITY_DN35322_c1_g2_i2	-2.9511	-1.3865	0.0003	0.0550	putative zinc finger protein 91 (Fragment)	2.00E-92	*Operophtera brumata*
TRINITY_DN30567_c6_g2_i1	-2.9059	-1.5217	0.0000	0.0093	-	-	-
TRINITY_DN34764_c2_g2_i9	-2.8990	-2.6731	0.0001	0.0237	-	-	-
TRINITY_DN39515_c0_g1_i5	-2.7516	1.2549	0.0001	0.0286	lachesin-like	0	*Bombyx mori*
TRINITY_DN33240_c0_g1_i6	-2.7220	-3.2631	0.0000	0.0017	uncharacterized protein	2.00E-120	*Bombyx mori*
TRINITY_DN29565_c0_g2_i1	-2.6506	-1.7899	0.0000	0.0045	-	-	-
TRINITY_DN35544_c0_g3_i2	-2.6469	-0.4176	0.0000	0.0098	UPF0528 protein CG10038	6.00E-55	*Amyelois transitella*
TRINITY_DN38353_c3_g1_i8	-2.6247	-3.0481	0.0001	0.0232	-	-	-
TRINITY_DN38108_c0_g2_i6	-2.6245	2.6610	0.0000	0.0100	uncharacterized protein LOC106136039	2.00E-152	*Amyelois transitella*
TRINITY_DN31477_c2_g1_i3	-2.5817	-0.6315	0.0000	0.0034	-	-	-

Table 3 continued.

Transcript ID	Log_2 Fold Change	Ave. Expression	P Value	FDR-Adjusted P Value	Top UniRef90 BLASTX Hit	E-value	Organism
TRINITY_DN30567_c9_g1_i1	-2.5463	-1.0038	0.0000	0.0030	-	-	-
TRINITY_DN39985_c0_g1_i3	-2.5356	5.1760	0.0000	0.0027	histone-lysine N-methyltransferase ash1	0	*Papilio* sp.
TRINITY_DN31213_c0_g1_i2	-2.4078	0.6190	0.0002	0.0472	GDNF-inducible zinc finger protein 1-like	9.00E-157	*Papilio* sp.
TRINITY_DN38047_c1_g1_i5	-2.2382	1.4642	0.0000	0.0068	uncharacterized protein	6.00E-112	*Obtectomera* sp.
TRINITY_DN37035_c0_g10_i2	-2.1924	3.4328	0.0001	0.0339	-	-	-
TRINITY_DN37004_c7_g1_i3	-2.1562	-2.1811	0.0000	0.0133	-	-	-
TRINITY_DN39427_c3_g1_i2	-2.0552	-0.3606	0.0002	0.0488	zinc finger protein 62 homolog isoform X2	2.00E-81	*Amyelois transitella*
TRINITY_DN31830_c4_g3_i2	-1.7960	-3.7434	0.0000	0.0043	mucin-2-like	1.00E-59	*Amyelois transitella*
TRINITY_DN39449_c0_g1_i14	-1.7253	-3.5318	0.0001	0.0207	uncharacterized protein	0	*Obtectomera* sp.
TRINITY_DN36559_c0_g2_i7	-1.7199	-0.8964	0.0001	0.0327	uncharacterized protein	2.00E-44	*Danaus plexippus*
TRINITY_DN38544_c0_g3_i1	-1.7008	-1.8335	0.0002	0.0488	-	-	-
TRINITY_DN38707_c1_g2_i9	-1.6822	2.9542	0.0001	0.0237	cytochrome P450 9A58	1.00E-166	*Spodoptera frugiperda*
TRINITY_DN37901_c0_g1_i4	-1.6242	1.0172	0.0001	0.0207	uncharacterized protein LOC106132143	0	*Amyelois transitella*
TRINITY_DN37610_c5_g1_i3	-1.6189	0.6339	0.0001	0.0332	uncharacterized protein LOC105397907	4.00E-92	*Plutella xylostella*
TRINITY_DN37496_c0_g2_i3	-1.5968	1.2808	0.0001	0.0178	uncharacterized protein	5.00E-97	*Danaus plexippus*
TRINITY_DN32710_c0_g1_i1	-1.5769	2.2427	0.0001	0.0264	uncharacterized protein	0	*Danaus plexippus*
TRINITY_DN39385_c2_g1_i5	-1.5003	5.7753	0.0001	0.0202	-	-	-
TRINITY_DN22676_c0_g1_i1	-1.4828	-0.6327	0.0001	0.0251	-	-	-

Table 4. List of statistically over-represented (hypergeometric test, FDR-adj. $p < 0.05$) Gene Ontology (GO) term annotations associated with the 290 differentially-expressed (DE) transcripts identified after frequent, prolonged bat-ultrasound exposure in brain tissue of adult male *Spodoptera frugiperda* moths.

GO Category	GO ID	Description	DE Cluster Frequency	GO-Annotated Transcriptome Frequency	FDR-Adjusted P Value
Biological Process	6536	glutamate metabolic process	3/102 (2.9%)	10/40511 (0.1%)	1.84E-06
	6537	glutamate biosynthetic process	3/102 (2.9%)	10/40511 (0.1%)	1.84E-06
	43650	dicarboxylic acid biosynthetic process	3/102 (2.9%)	21/40511 (0.1%)	1.99E-05
	7229	integrin-mediated signaling pathway	4/102 (3.9%)	89/40511 (0.1%)	7.85E-05
	43648	dicarboxylic acid metabolic process	3/102 (2.9%)	53/40511 (0.1%)	3.31E-04
	9084	glutamine family amino acid biosynthetic process	3/102 (2.9%)	64/40511 (0.1%)	5.77E-04
Molecular Function	3682	chromatin binding	7/102 (6.8%)	77/40511 (0.1%)	1.08E-09
	44877	macromolecular complex binding	7/102 (6.8%)	135/40511 (0.1%)	5.54E-08
	15930	glutamate synthase activity	3/102 (2.9%)	5/40511 (0.1%)	1.54E-07
	45181	glutamate synthase activity, NAD(P)H as acceptor	2/102 (1.9%)	4/40511 (0.1%)	3.75E-05
	16040	glutamate synthase (NADH) activity	2/102 (1.9%)	4/40511 (0.1%)	3.75E-05
	10181	FMN binding	3/102 (2.9%)	49/40511 (0.1%)	2.62E-04
	16639	oxidoreductase activity, acting on the CH-NH2 group of donors, NAD or NADP as acceptor	2/102 (1.9%)	11/40511 (0.1%)	3.40E-04
	16638	oxidoreductase activity, acting on the CH-NH2 group of donors	3/102 (2.9%)	55/40511 (0.1%)	3.70E-04
	4046	aminoacylase activity	2/102 (1.9%)	12/40511 (0.1%)	4.08E-04

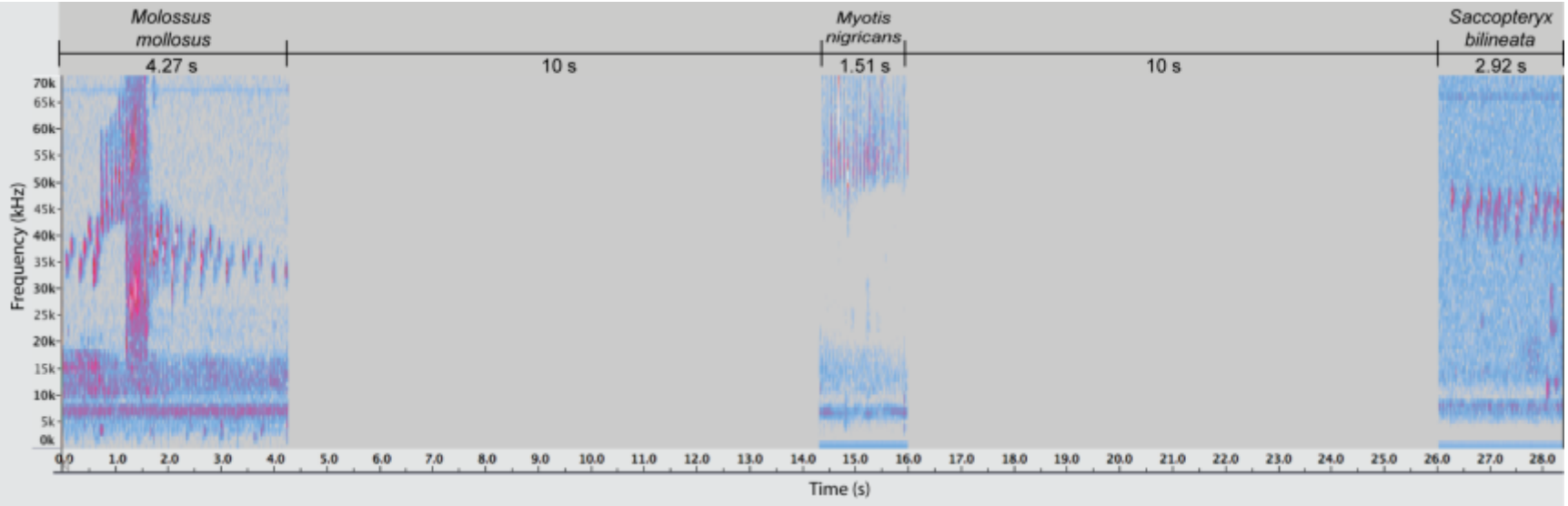

Figure 1. Truncated spectrogram detailing the frequencies and time of the .wav bat-ultrasound recordings used during predator-cue exposure trials, with the final 10 s of silence in each loop not shown; each call is labelled with the species of bat the call was recorded from and its length in time.

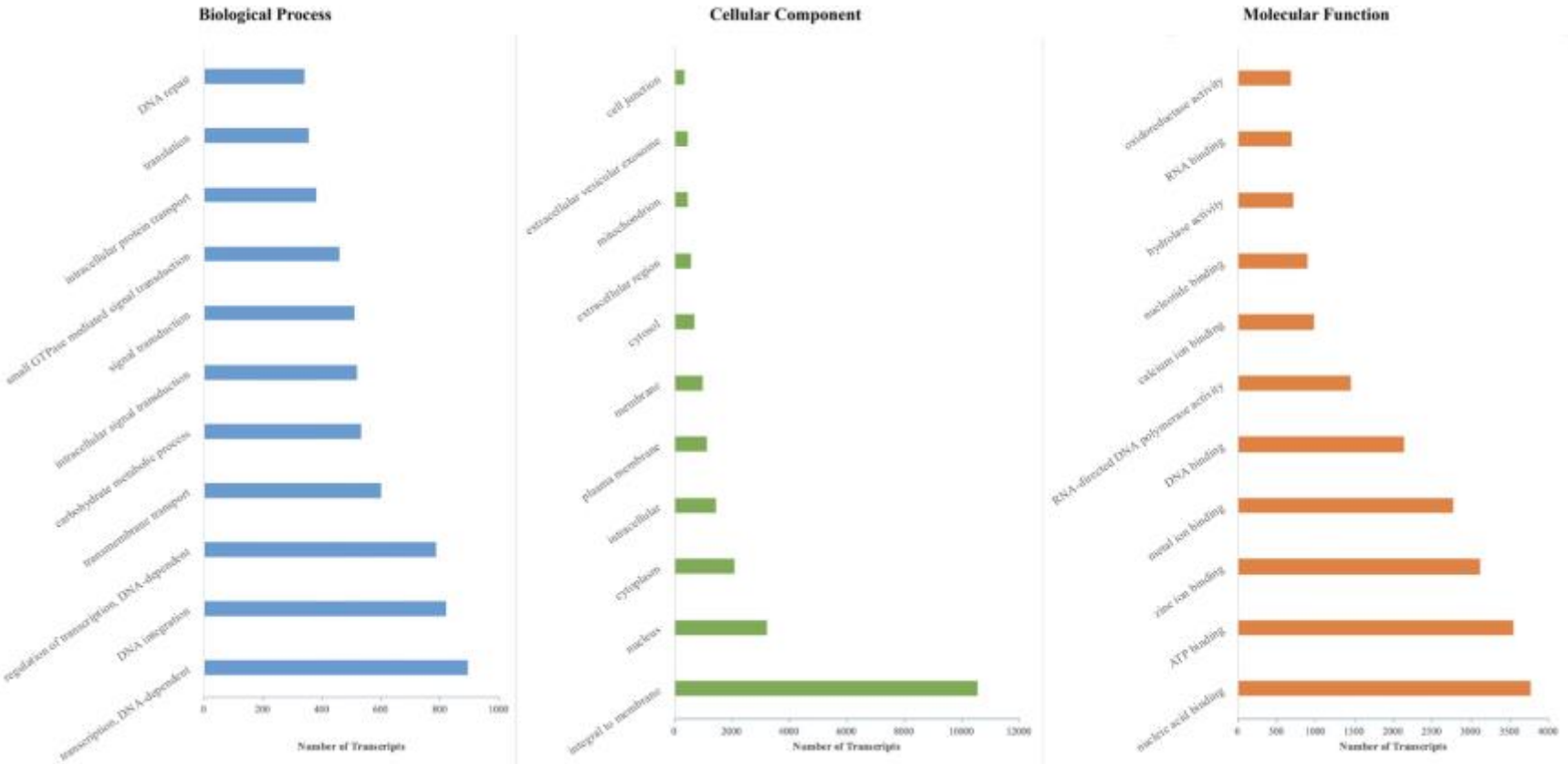

Figure 2. Top 10 Gene Ontology (GO) term annotations and their abundance represented in our *de novo* transcriptome constructed from brain tissue of both control and bat-ultrasound exposed adult male *Spodoptera frugiperda* within each of three GO categories: biological process, cellular component, and molecular function.

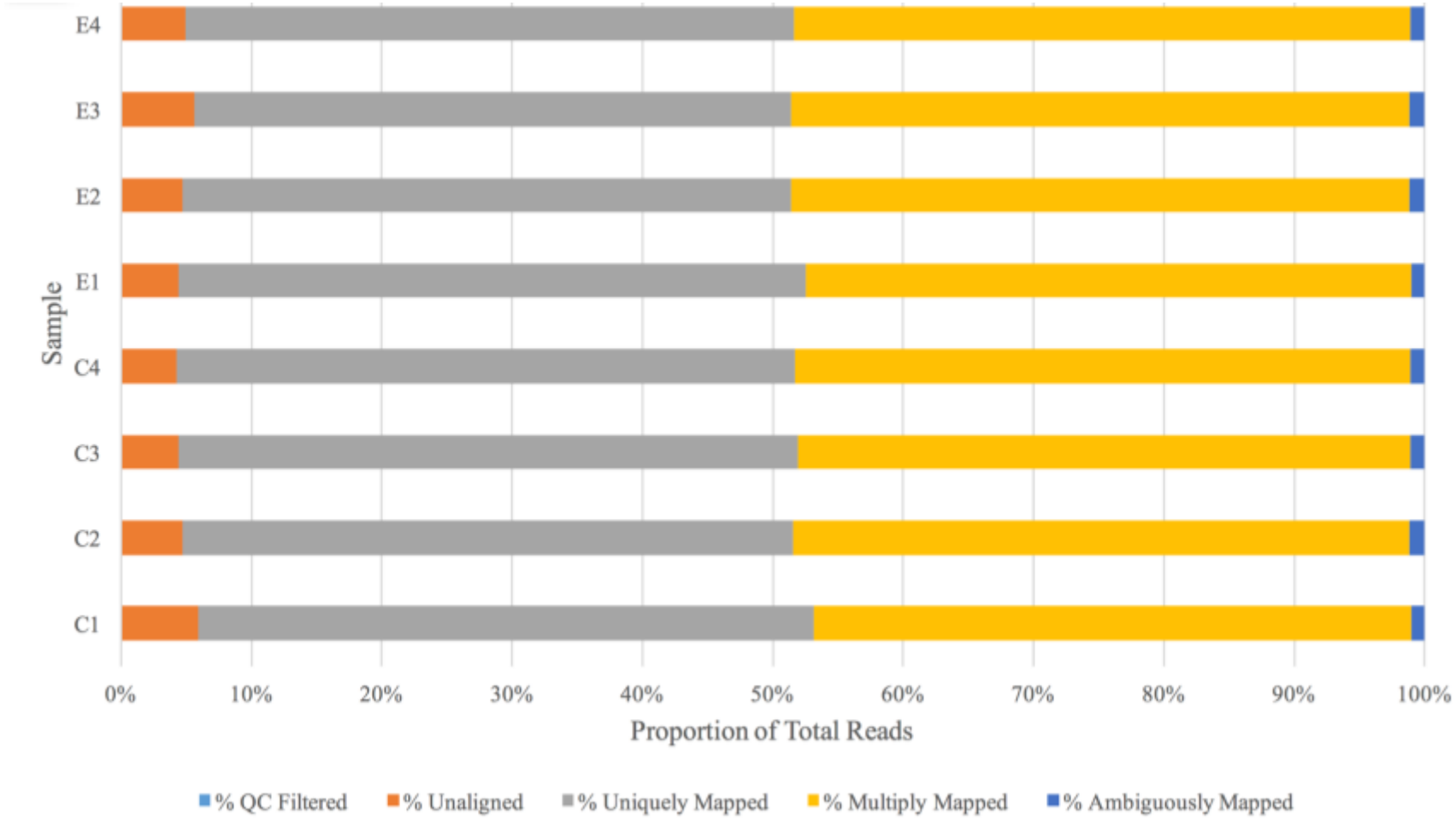

Figure 3. mRNA read fates after alignment to our *de novo* assembled transcriptome pertaining to control (C) and exposed (E) *Spodoptera frugiperda* adult male moth brain tissue sequences; QC = quality checked.

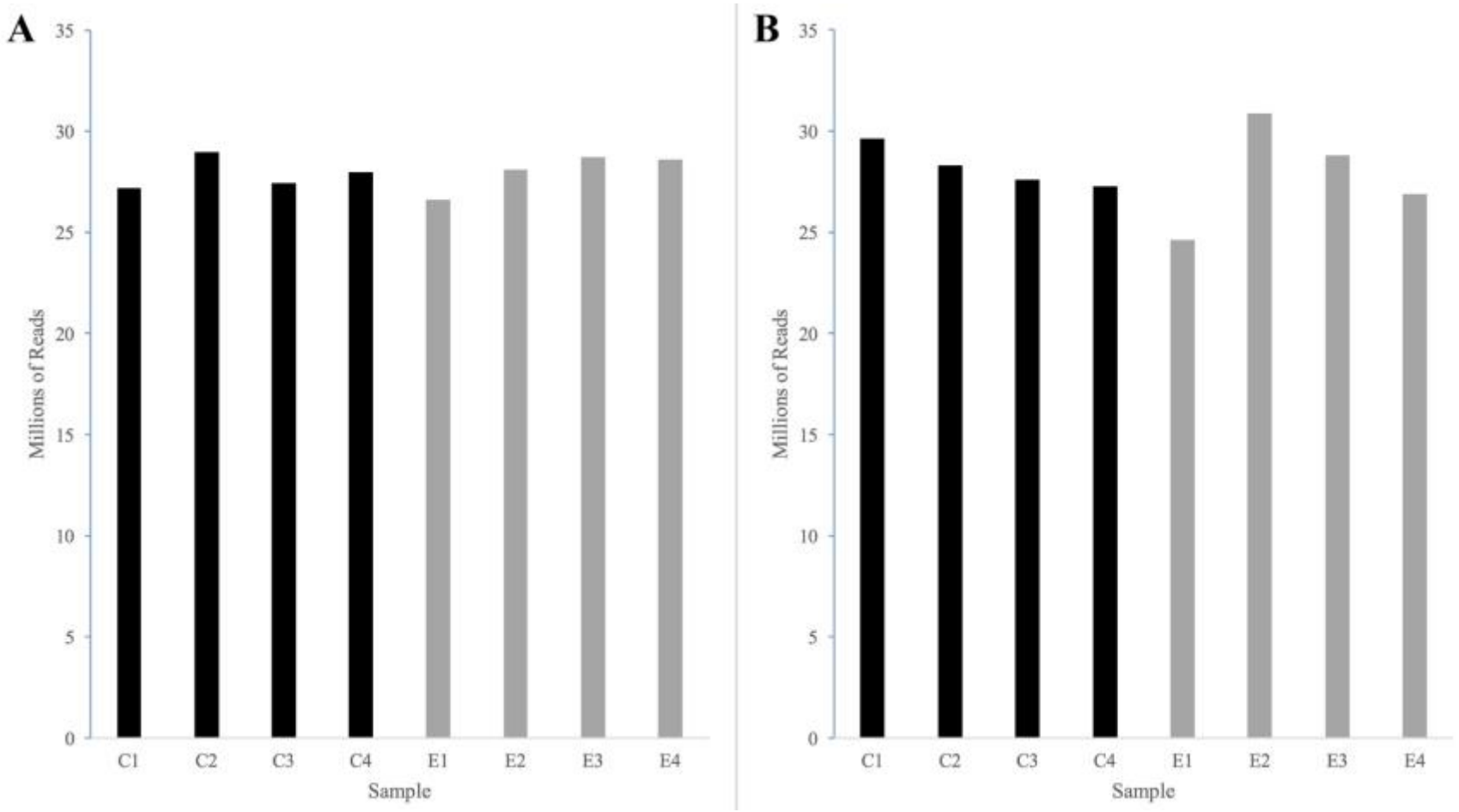

Figure 4. Actual (A) and TMM normalized effective (B) mRNA read library sizes recovered from the brains of both control (C) and exposed (E) adult male *Spodoptera frugiperda* moths.

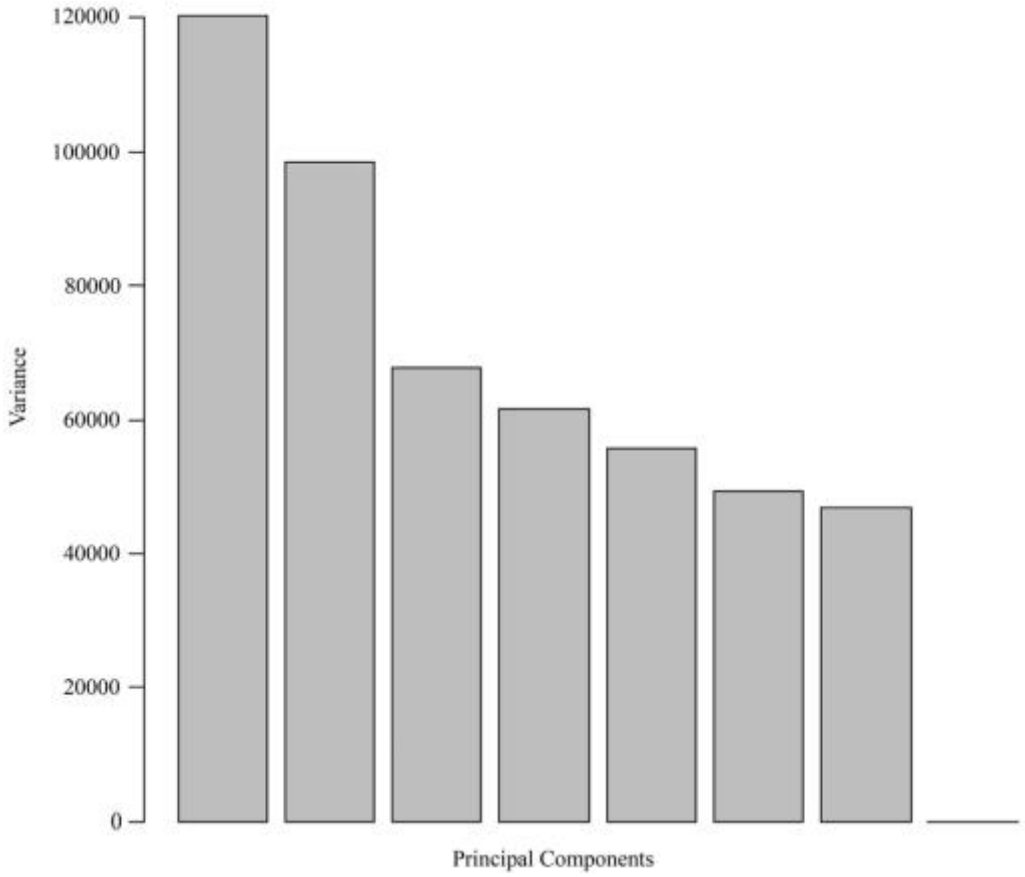

Figure 5. Scree plot indicating the transcript expression variances, estimated using log-based counts per million reads, corresponding to the first eight principal components identified.

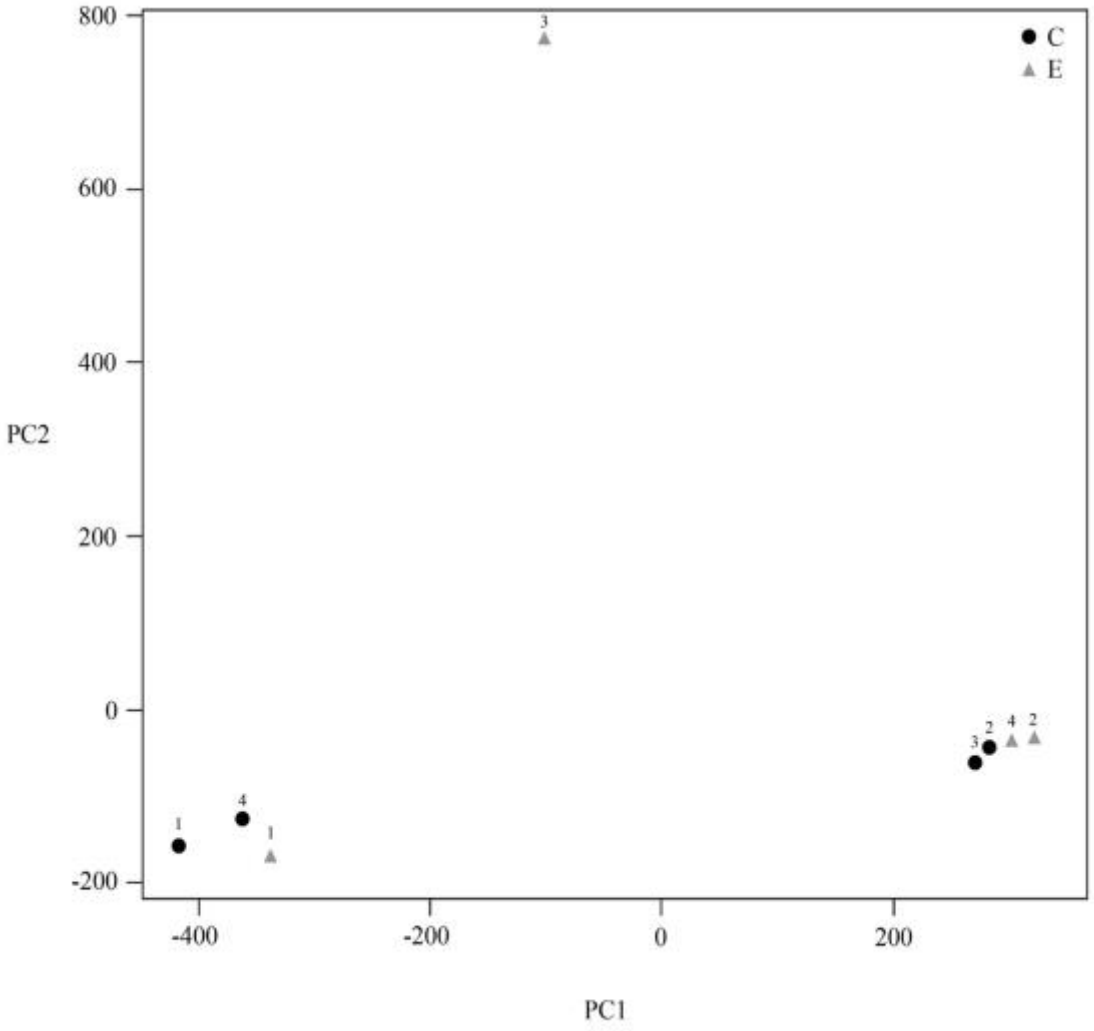

Figure 6. Principal components plot showing sample clustering based on the first two principal components of variation in log-based counts per million read estimates for both control (C; black circle) and bat-ultrasound exposed (E; grey triangle) *Spodoptera frugiperda* moths; numbers (1-4) represent replicate samples from each of the control and exposure groups.

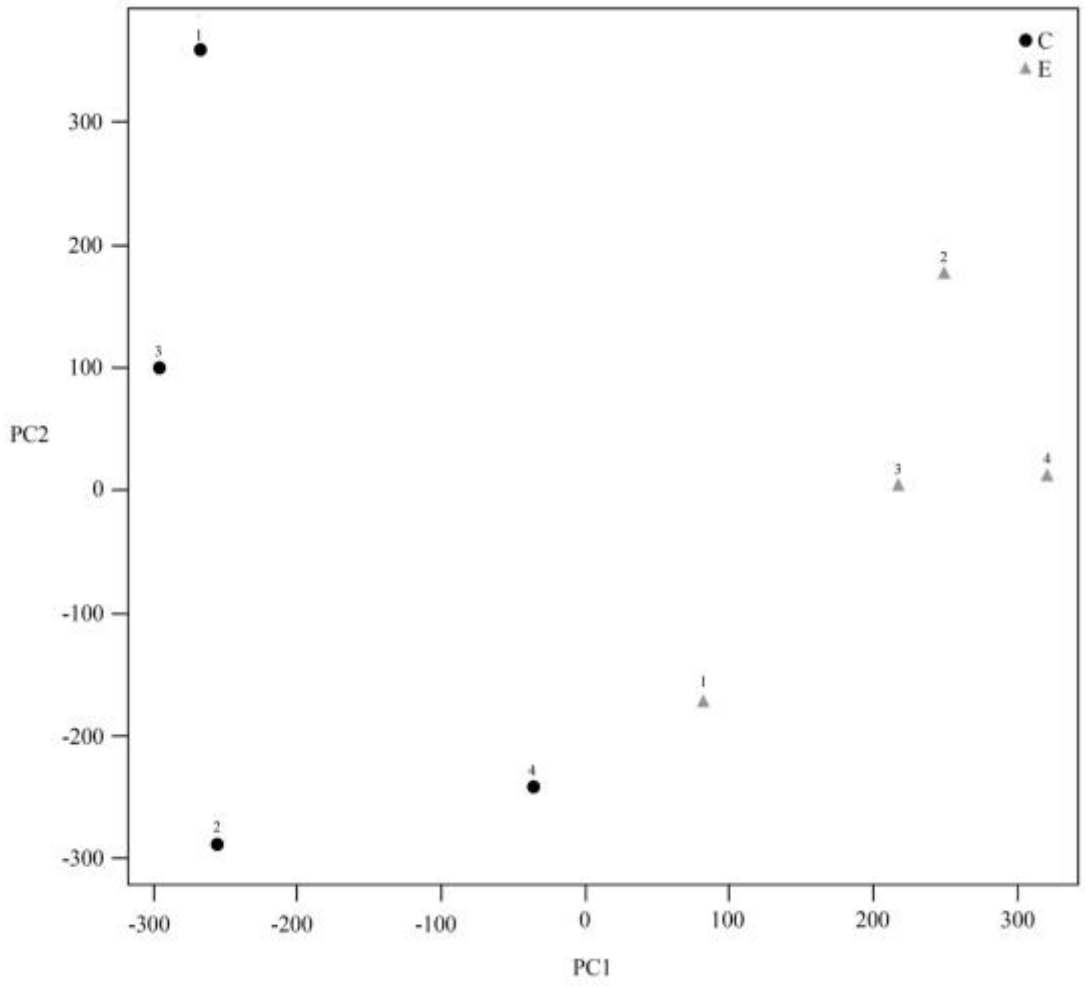

Figure 7. Principal components plot after surrogate variable analysis was performed to account for unexpected batch effects showing sample clustering based on the first two principal components of variation in log-based counts per million read estimates for both control (C; black circle) and bat-ultrasound exposed (E; grey triangle) adult male *Spodoptera frugiperda* moths; numbers (1-4) represent replicate samples from each of the control and exposure groups.

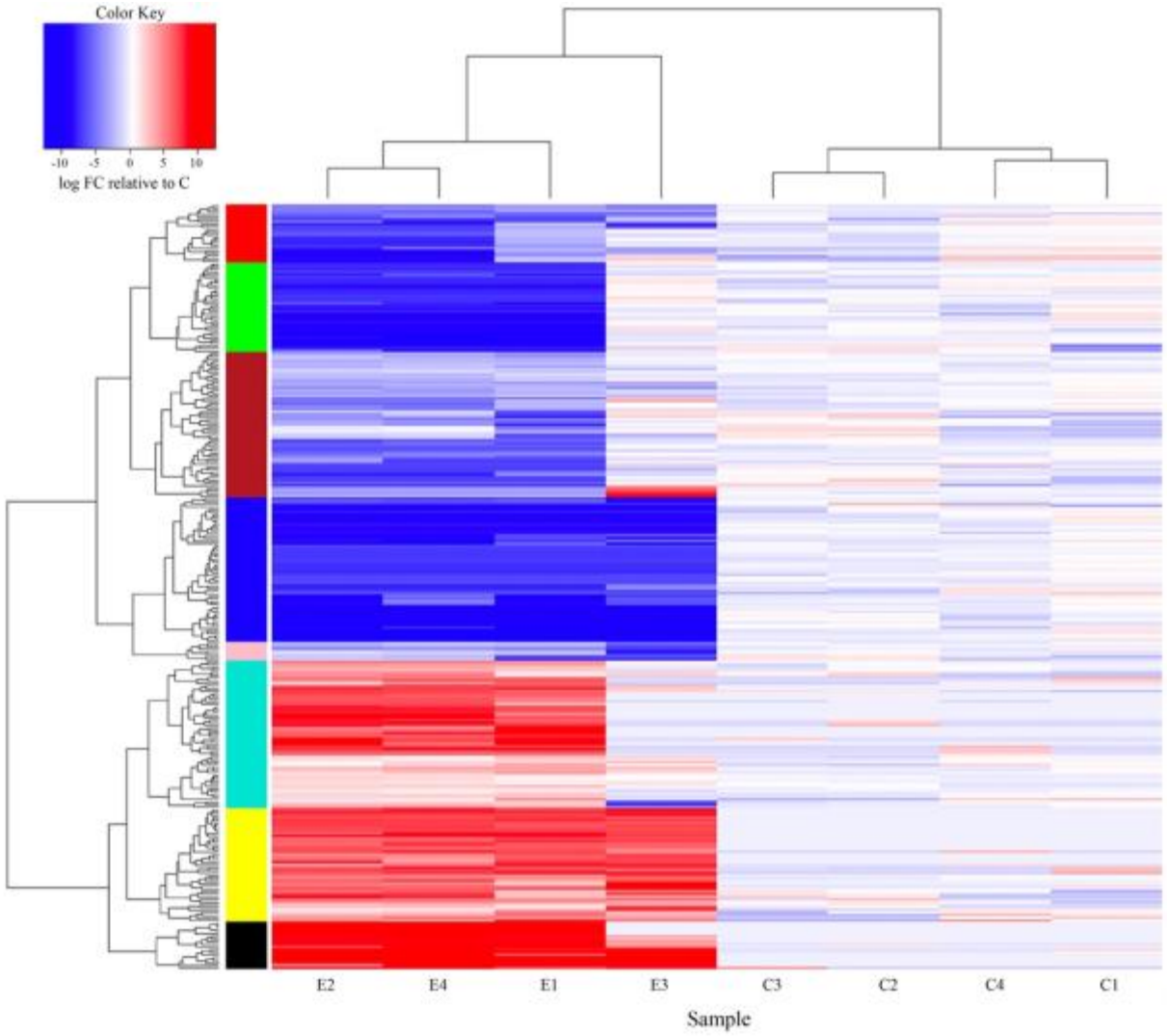

Figure 8. Transcript expression heatmap detailing the up- (red) and down- (blue) regulation (log_2 fold-change) of each transcript relative to the mean expression of the control group across both control (C) and bat-ultrasound exposed (E) adult male *Spodoptera frugiperda* moths; samples (horizontal axis) and transcripts (vertical axis) are clustered according to expression similarity.